Photon Statistics and Quantum Properties of a Cascade Three-Level Atomic System Coupled to a Two-Mode Squeezed-Vacuum Reservoir in the Bad-Cavity Limit.

Adagn Addisu Dabulo[1] and Misrak Getahun[2]*
[1]*Department of Physics, Hawassa University, P.O.Box 05, Hawassa, Ethiopia*
[2]*Department of Physics, Hawassa University, P. O. Box 05, Hawassa, Ethiopia*
(Dated: September 9, 2026)

Abstract: We investigate the steady-state photon statistics and quantum properties of a cascade three-level atom coupled to a two-mode squeezed-vacuum reservoir. The mean photon number, photon-number correlations, second-order coherence, and quadrature fluctuations are examined as functions of the stimulated-emission decay constant and the squeezing parameter. The system exhibits two distinct regimes: a squeezing-dominated regime, governed by reservoir-induced correlations, and a cavity-dynamics-dominated regime, characterized by strong gain–loss competition. Enhanced squeezing increases photon generation, intermodal correlations, and intracavity energy through correlated photon-pair injection while reducing vacuum fluctuations. Conversely, stronger stimulated emission induces nonlinear amplification, asymmetric photon distributions, and sequential emission dynamics. A transition from super-Poissonian to sub-Poissonian statistics is observed, indicating the coexistence of photon antibunching and continuous-variable quantum correlations. Furthermore, atom–cavity interactions modify the generalized uncertainty bounds, revealing fundamental limitations on achievable squeezing imposed by higher-order noise processes. These findings demonstrate that engineered reservoirs and cascade atomic systems provide versatile control of nonclassical light for quantum communication, precision metrology, and continuous-variable quantum information processing.

Keywords: Squeezed vacuum radiation; Non-classical light; Quadrature squeezing; Squeeze parameter.

DOI:

PACS numbers: 42.50.-p, 42.50.Dv, 42.50.Lc, 42.50.Wk

1. Introduction

Quantum optics is the union of quantum field theory and physical optics,to study the time evolution of the system. The subject evolved from early studies of the coherence properties of radiation and the fundamental principles underlying laser operation. It has since expanded to encompass modern research directions, including the study of three-level atoms, squeezed states of the light field, and atomic coherence. These topics remain highly relevant to the reduction of quantum noise in interferometry and the development of optical amplifiers[1],[2]. A three-level atom is a fundamental quantum-optical system in which the interaction between its discrete energy levels and an electromagnetic field can give rise to light emission, while its coupling to the surrounding vacuum reservoir governs its spontaneous-emission dynamics. When a three-level atom transitions from the top to the bottom via the intermediate level, two photons are emitted given as Fig. 1. The two photons are highly correlated and this correlation is responsible for the squeezing of the light produced by a three-level atom. Quantum optics is a field of quantum physics that deals mainly the quantum properties of light generated by various quantum optical system such as lasers and with the effect of light on the dynamics of atoms[3],[4].

Quantum optics provides a powerful new probe for addressing fundamental issues in quantum mechanics such as complementarity, hidden variables, and other aspects that are central to the foundation of quantum physics and philosophy. For the description of a quantum system, the concept of state is used, which is the same, a wave function, a state vector or density matrix, quasi-probability distribution containing the information about the possible results of measurement on the system. Furthermore, quantum optics has statistical origin and therefore the state of quantum system contains all information necessary to completely determine its statistics (the probabilistic nature of a quantum system)[1],[2],[3],[5].

In quantum theory, light is composed of particles called photons, and the properties of light are described in terms of the creation and annihilation operators of photons in the quantum state. The quantum properties of light are largely determined by the state of the light mode, and the most important quantum states of light are the number and chaotic, coherent, and squeezed states. In a chaotic state, the variance of the photon number is greater than

*E-mail me at: adagna@hu.edu.et/adagnaddisu@gmail.com

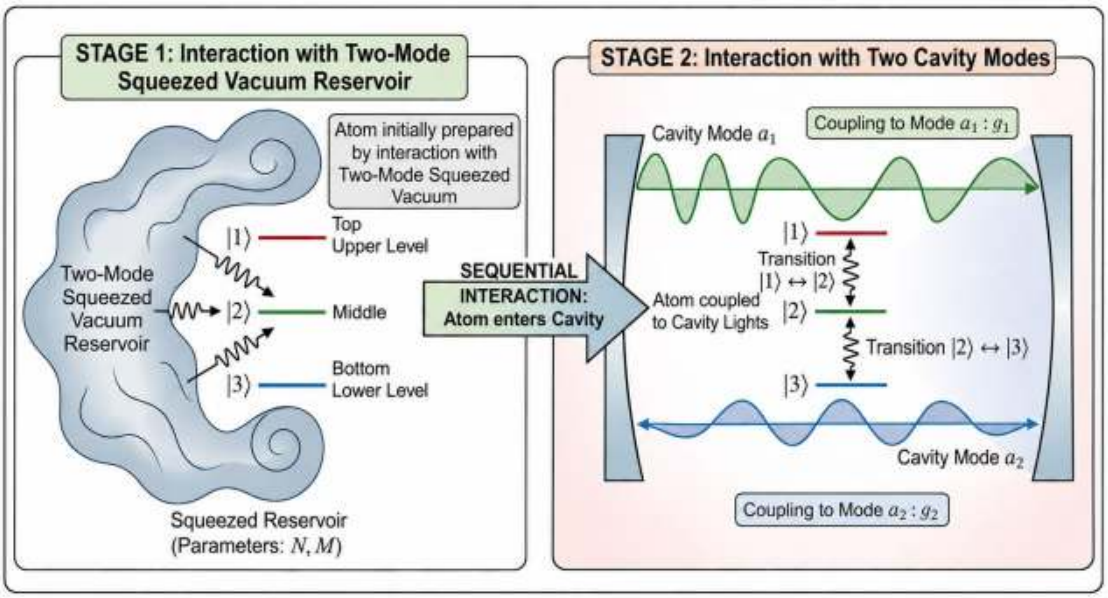


FIG. 1: Schematic diagram of the system under consideration of a cascade three-level atom with states $|1\rangle$, $|2\rangle$, and $|3\rangle$ interacts with two cavity modes a_1 and a_2, corresponding to the transitions $|1\rangle \leftrightarrow |2\rangle$ and $|2\rangle \leftrightarrow |3\rangle$, respectively; coupled to a squeezed vacuum reservoir characterized by the parameters N and M

.

the mean photon number, and the radiation exhibits super-Poissonian statistics. The coherent state is a specific superposition of number states. In contrast to a number state, a coherent state does not possess a definite number of photon the photon distribution is Poissonian. The coherent state is a special minimum uncertainty state. In number state or fock state the variance of photon numbers is zero, the radiation has sub-posissonian statics and they are useful representation of high energy photons. Number states and squeezed state are further typical example of non-classical states[1]–[3],[5]–[7].

Squeezed state is a state of light that can be defined in terms of hermitian plus and minus quadrature operators, in which the fluctuation in one quadrature is below the coherent or vacuum level at the expense of enhanced fluctuation in the other quadrature with the product of uncertainties in the two quadratures satisfying the uncertainty relation. In addition to exhibiting a non classical feature, squeezed light has potential applications in the detection of weak signal and in low noise communications[2],[3],[5],[7]–[16].

1.1. Master Equation of Cascade Three-Level Atom

In this section we wish to derive the master equation representing the interaction of three-level atoms in cascade configuration with a two-mode squeezed radiation inside the cavity and the cavity modes are also coupled to vacuum reservoir. The dynamics of a quantum system can be portrayed by time evolution of the reduced density operator that often dubbed as master equation. One may note that the cavity can also interact with the environment via the exchange of fluctuations that requires the cavity to be at equilibrium with the surrounding enclosure before the commencement of the interaction[2]. Starting from the full dipole interaction Hamiltonian containing terms of the form $(\hat{a}_i + \hat{a}_i^\dagger)(\hat{\sigma}_{jk} + \hat{\sigma}_{kj})$, one obtains both energy-conserving and counter-rotating contributions. In the interaction picture, these terms oscillate at frequencies $\omega_i - \omega_{jk}$ and $\omega_i + \omega_{jk}$, respectively. The counter-rotating terms, $\hat{a}_i\hat{\sigma}_{jk}$ and $\hat{a}_i^\dagger\hat{\sigma}_{kj}$, oscillate rapidly at frequencies $\sim (\omega_i + \omega_{jk})$, and therefore average out over the relevant timescale. Under the rotating-wave approximation (RWA), these terms are neglected, leaving only the energy-conserving terms $\hat{a}_i\hat{\sigma}_{kj}$ and $\hat{a}_i^\dagger\hat{\sigma}_{jk}$. This approximation is valid in the near-resonant weak-coupling regime, where the atom–field coupling strength satisfies $g_i \ll \omega_i, \omega_{jk}$, and the detuning $|\omega_i - \omega_{jk}|$ is much smaller than the optical frequencies. Under these conditions, the Hamiltonian reduces to the standard Jaynes–Cummings interaction widely used in quantum optics. The interaction three-level cascade Hamiltonian under RWA explicitly as:

$$\hat{H}_{AC} = ig\left(\hat{\sigma}_{12}\hat{a}_1 - \hat{a}_1^\dagger\hat{\sigma}_{21} + \hat{\sigma}_{23}\hat{a}_2 - \hat{a}_2^\dagger\hat{\sigma}_{32}\right), \tag{1}$$

where $\hat{\sigma}_{12} = |1\rangle\langle 2|$ ($\hat{\sigma}_{21} = |2\rangle\langle 1|$) and $\hat{\sigma}_{23} = |2\rangle\langle 3|$ ($\hat{\sigma}_{32} = |3\rangle\langle 2|$) are atomic rising (lowering) operators, $\hat{a_1}$ ($\hat{a_1}^\dagger$) and $\hat{a_2}$ ($\hat{a_2}^\dagger$) are the annihilation (creation) operators for cavity modes and g is the coupling constant between the atom and cavity modes. Consider two reservoir continua described by the operators $\hat{c}_k$, $\hat{d}_k$ with the reservoir Hamiltonian

of:

$$\hat{H}_R = \sum_k \hbar\omega_{c,k}\hat{c}_k^\dagger\hat{c}_k + \sum_k \hbar\omega_{d,k}\hat{d}_k^\dagger\hat{d}_k. \tag{2}$$

The reservoir is prepared in a broadband two-mode squeezed vacuum state

$$|\Psi_R\rangle = \hat{S}_2(r,\phi)|0\rangle, \tag{3}$$

for

$$\hat{S}_2(r,\phi) = \exp\left[r\left(e^{-i\phi}\hat{c}\hat{d} - e^{i\phi}\hat{c}^\dagger\hat{d}^\dagger\right)\right]. \tag{4}$$

Where the complex squeezing parameter $M = |M|e^{i\phi}$, and the reservoir does not contain independent vacuum modes instead, photons are generated in correlated pairs, whenever one photon appears in mode c, another appears simultaneously in mode d nonlinear process such as nondegenerate parametric down-conversion inside a $\chi^{(2)}$ crystal creates photon pairs. The two transitions interacting with the reservoir become correlated through the common pair-generation process. We consider the reservoir to be composed of a large number of submodes the interaction between the atomic transitions and the squeezed vacuum reservoir is described by the Hamiltonian

$$\hat{H}_{AR}(t) = i\sum_k \lambda_k\left(\hat{\sigma}_{12}\hat{c}_k e^{i\omega_{1k}t} - \hat{c}_k^\dagger\hat{\sigma}_{21}e^{-i\omega_{1k}t}\right) + i\sum_k \lambda_k\left(\hat{\sigma}_{23}\hat{d}_k e^{i\omega_{2k}t} - \hat{d}_k^\dagger\hat{\sigma}_{32}e^{-i\omega_{2k}t}\right), \tag{5}$$

where ω_k denotes the reservoir-mode frequency, ω_1 and ω_2 are the atomic transition frequencies, λ_k is the atom–reservoir coupling constant (assumed identical for both transitions), and $\hat{c}_k$ and $\hat{d}_k$ are the annihilation operators associated with the reservoir submodes. The detunings are defined by $\omega_{1k} = \omega_1 - \omega_k$ and $\omega_{2k} = \omega_2 - \omega_k$. Assume that the squeezing is broadband, correlation time of the squeezed bath is given by $\tau_s \sim \frac{1}{\Delta\omega_s}$. Since $\Delta\omega_s \gg \gamma, \kappa, g$, it follows that$\tau_s \ll \frac{1}{\gamma}, \frac{1}{\kappa}, \frac{1}{g}$ therefore, the bath loses its memory almost immediately. Where $\Delta\omega_s$ is the squeezing bandwidth, γ is the atomic decay rate, κ is the cavity decay rate, and g is the coherent coupling strength. Under this condition, the spectrum of the squeezed reservoir is extremely broad compared with all relevant system frequency scales, and the reservoir responds almost instantaneously. This behavior arises because the nonlinear source generates squeezing over a very large frequency interval, causing the reservoir to possess essentially no memory. This is because a broad spectrum in the frequency domain corresponds, through the Fourier transform, to a narrow correlation function in the time domain. Consequently, the system never experiences the bath's past history, which provides the fundamental physical justification for the Markov approximation and the use of Lindblad master equations. The fluctuating reservoir forces are

$$\hat{F}_c(t) = \sum_k g_k^c\hat{c}_k e^{-i(\omega_k-\omega_c)t}, \quad \hat{F}_d(t) = \sum_k g_k^d\hat{d}_k e^{-i(\omega_k-\omega_d)t}, \tag{6}$$

where g_k^c and g_k^d represent the frequency-dependent coupling constants between the system and the k-th submode of the c and d reservoir continua, respectively. These coupling strengths are intrinsically related to the interaction parameter λ_k introduced in Eq. (5). Together, these operators represent the random quantum fluctuations exerted by the squeezed vacuum on the system. Each reservoir mode contributes a small fluctuating field, and the total noise is obtained by summing over all modes. This noise drives spontaneous emission, decoherence, and squeezed-noise-induced effects. For a two-mode squeezed vacuum, the reservoir moments are characterized by

$$N = \sinh^2 r, \qquad M = \sinh r\cosh r, \tag{7}$$

and the nonzero phase-sensitive correlations satisfy

$$\begin{aligned}\langle\hat{c}_k\hat{d}_{k'}\rangle &= Me^{i\phi}\delta_{kk'}\\ \langle\hat{c}_k^\dagger\hat{d}_{k'}^\dagger\rangle &= Me^{-i\phi}\delta_{kk'}.\end{aligned} \tag{8}$$

Because these are pair correlations, they indicate that photons in modes c and d are created simultaneously. Both photons originate from the same down-conversion event. Consequently, the reservoir couples two otherwise independent transitions. By substitute the noise operators calculate $\langle F_c^\dagger(t)F_c(t')\rangle$ as:

$$\langle F_c^\dagger(t)F_c(t')\rangle = \sum_{kk'} g_k^{c*}g_{k'}^c e^{i(\omega_k-\omega_c)t}e^{-i(\omega_{k'}-\omega_c)t'}\langle c_k^\dagger c_{k'}\rangle. \tag{9}$$

Using $\langle c_k^\dagger c_{k'}\rangle = N\delta_{kk'}$, gives

$$\langle F_c^\dagger(t)F_c(t')\rangle = N\sum_k |g_k^c|^2 e^{i(\omega_k-\omega_c)(t-t')}. \tag{10}$$

This quantity measures the intensity fluctuations supplied by the squeezed bath. The bath contains, on average, N photons. As a result, stimulated processes accompany spontaneous emission, leading to modifications of the decay rates and fluorescence spectra. Replace the mode sum by a continuum due to Born-Markov approximation :

$$\sum_k |g_k|^2 \to \int d\omega, D(\omega)|g(\omega)|^2. \tag{11}$$

Assume $D(\omega)|g(\omega)|^2 = \frac{\Gamma}{2\pi}$ is approximately constant across the squeezing bandwidth. Then

$$N\frac{\Gamma}{2\pi}\int_{-\infty}^{\infty} d\omega e^{i(\omega-\omega_c)(t-t')}. \tag{12}$$

Using $\int_{-\infty}^{\infty} e^{ix\tau}dx = 2\pi\delta(\tau)$, we obtain

$$\langle F_c^\dagger(t)F_c(t')\rangle = N\Gamma\delta(t-t'). \tag{13}$$

Noise at different times is uncorrelated because $\tau_s \ll \tau_{\text{system}}$, for τ_s is the bath correlation time and τ_{system} is the characteristic system timescale. Consequently, the bath loses its memory almost instantaneously, exhibits white-noise statistics, and possesses the cross-correlation $\langle F_c(t)F_d(t')\rangle$ given by:

$$\langle F_c(t)F_d(t')\rangle = \sum_{kk'} g_k^c g_{k'}^d e^{-i(\omega_k-\omega_c)t}e^{-i(\omega_{k'}-\omega_d)t'}\langle c_k d_{k'}\rangle. \tag{14}$$

Substituting $\langle c_k d_{k'}\rangle = Me^{i\phi}\delta_{kk'}$ yields:

$$\langle F_c(t)F_d(t')\rangle = Me^{i\phi}\sum_k g_k^c g_k^d e^{-i(\omega_k-\omega_c)t}e^{-i(\omega_k-\omega_d)t'}. \tag{15}$$

Applying the same Markov approximation gives

$$\langle F_c(t)F_d(t')\rangle = Me^{i\phi}\Gamma\delta(t-t'), \quad \langle F_c^\dagger(t)F_d^\dagger(t')\rangle = Me^{-i\phi}\Gamma\delta(t-t'). \tag{16}$$

The condition $\langle F_c(t)F_d(t')\rangle \neq 0$ implies that the noise acting on one transition is correlated with the noise acting on the other. These correlations depend on the squeezing phase ϕ. Physically, they arise because photon pairs are created coherently:

$$|0,0\rangle \to |1,1\rangle \to |2,2\rangle. \tag{17}$$

The two photons carry a definite phase relationship inherited from the pump field. As a result, the environment can transfer coherence and entanglement to the system. The bath no longer merely destroys quantum properties; it can also generate them. We carry out our calculation by putting noise operators associated with the vacuum reservoir in normal order. However, the inclusion of noise operators in the quantum Langevin formalism is essential for preserving the canonical commutation relations and ensuring consistency with the fluctuation–dissipation theorem. Although these operators do not contribute to normally ordered expectation values, they play a crucial role in determining higher-order correlations and quantum fluctuations. Using Eq. (1) and the relation

$$\frac{d\hat{A}}{dt} = -\frac{1}{2}\kappa\hat{A} - i\left[\hat{A}, \hat{H}_{AC}\right] + \hat{F}(t), \tag{18}$$

where $\hat{F}(t)$ is noise operator. Since the noise fluctuation is taken as an effective contribution of the reservoir that alters the cavity dynamics, the annihilation operator for the input mode can be expressed in terms of the noise operator and cavity damping constant as[2]

$$\hat{a}_{i,in}(t) = \frac{1}{\sqrt{\kappa}}\hat{F}_i(t). \tag{19}$$

The time development of the annihilation operator for the cavity radiation can thus be modified as

$$\frac{d\hat{a}_i}{dt} = -i[\hat{a}_i(t), \hat{H}_S(t)] - \frac{\kappa}{2}\hat{a}_i(t) + \sqrt{\kappa}\,\hat{a}_{i_i n}(t), \tag{20}$$

then the quantum Langevin equations for the cavity mode operators $\hat{a_1}$ and $\hat{a_2}$ can be written as

$$\frac{d\hat{a_1}}{dt} = -\frac{1}{2}\kappa\hat{a_1} - g\hat{\sigma}_{21} + \sqrt{\kappa}\hat{a}_{\mathrm{in},1}, \tag{21}$$

and

$$\frac{d\hat{a_2}}{dt} = -\frac{1}{2}\kappa\hat{a_2} - g\hat{\sigma}_{32} + \sqrt{\kappa}\hat{a}_{\mathrm{in},2}, \tag{22}$$

where κ is the cavity damping constant. We consider the atom interacts with a squeezed vacuum reservoir denoting the total density operator of the atomic system coupled to a squeezed vacuum reservoir by $\hat{\chi}(t)$, its time evolution is governed by the von Neumann equation

$$\frac{d\hat{\chi}(t)}{dt} = -i\left[\hat{H}_{AR}, \hat{\chi}(t)\right], \tag{23}$$

where $\hat{H}_{AR}$ is the interaction Hamiltonian describing the coupling between the atom and the reservoir. The reduced density operator of the atomic system is obtained by tracing over the reservoir degrees of freedom,

$$\hat{\rho}(t) = \mathrm{Tr}_R[\hat{\chi}(t)], \tag{24}$$

and therefore its equation of motion becomes

$$\frac{d\hat{\rho}(t)}{dt} = -i\,\mathrm{Tr}_R\left[\hat{H}_{AR}(t), \hat{\chi}(t)\right], \tag{25}$$

where Tr_R denotes the trace over the reservoir variables only. A formal integration of Eq. (23) yields

$$\hat{\chi}(t) = \hat{\chi}(0) - i\int_0^t \left[\hat{H}_{AR}(t'), \hat{\chi}(t')\right] dt'. \tag{26}$$

To proceed further, we employ the *Born approximation*, which assumes weak coupling between the atomic system and the reservoir. Under this assumption, the state of the reservoir remains essentially unaffected by the interaction and the total density operator factorizes as

$$\hat{\chi}(t') = \hat{\rho}(t')\hat{R}, \qquad \hat{\chi}(0) = \hat{\rho}(0)\hat{R}, \tag{27}$$

where $\hat{R}$ is the stationary density operator of the squeezed vacuum reservoir. Substituting Eq. (27) into Eq. (26), we obtain

$$\hat{\chi}(t) = \hat{\rho}(0)\hat{R} - i\int_0^t \left[\hat{H}_{AR}(t'), \hat{\rho}(t')\hat{R}\right] dt'. \tag{28}$$

Substituting Eq. (28) into Eq. (25) gives

$$\frac{d\hat{\rho}(t)}{dt} = -i\left[\langle\hat{H}_{AR}(t)\rangle_R, \hat{\rho}(0)\right] - \int_0^t \mathrm{Tr}_R\left[\hat{H}_{AR}(t), \left[\hat{H}_{AR}(t'), \hat{\rho}(t')\hat{R}\right]\right] dt', \tag{29}$$

where

$$\langle\hat{H}_{AR}(t)\rangle_R = \mathrm{Tr}_R\left[\hat{H}_{AR}(t)\hat{R}\right]. \tag{30}$$

It should be noted that, in addition to the Born approximation, the derivation implicitly relies on the *Markov approximation*. The Markov approximation assumes that the reservoir correlation time τ_R is much shorter than the characteristic timescale of the system τ_S, namely $\tau_R \ll \tau_S$, so that the reservoir possesses no memory of its past interactions with the system. Furthermore, the squeezed vacuum reservoir is assumed to satisfy the

broadband squeezing approximation. Since the reservoir modes are prepared in a two-mode squeezed vacuum state with nonvanishing correlations,

$$\langle \hat{c}_k \hat{d}_k \rangle \neq 0, \tag{31}$$

the validity of the Markov approximation requires the squeezing bandwidth $\Delta\omega_s$ to be much larger than all relevant system frequencies. Consequently, the reservoir correlation functions decay rapidly and can be approximated by delta functions, specifically $\Delta\omega_s \gg \max(\gamma, \kappa, g)$ where γ denotes the atomic decay rate, κ is the cavity damping constant, and g is the atom–field coupling strength. Under this condition, the reservoir correlation time $\tau_s \sim \frac{1}{\Delta\omega_s}$ becomes much smaller than the characteristic system timescales, $\tau_s \ll \tau_{\text{system}}$ and the reservoir correlations reduce to the delta-correlated form

$$\langle \hat{R}(t)\hat{R}(t') \rangle \propto \delta(t - t'). \tag{32}$$

Hence, the broadband squeezing assumption provides the physical justification for the Markov approximation and ensures a time-local master equation. If the squeezing bandwidth were comparable to or smaller than the system frequencies, the reservoir correlations would decay over a finite timescale,

$$\langle \hat{R}(t)\hat{R}(t') \rangle \sim e^{-|t-t'|/\tau_s}, \tag{33}$$

leading to non-Markovian memory effects and a nonlocal master equation. This property is reflected later in the reservoir correlation relations Eqs. (52)–(56), where the reservoir operators satisfy delta-correlated noise relations such as

$$\langle \hat{c}_k(t)\hat{c}_k^{\dagger}(t') \rangle \propto \delta(t - t'). \tag{34}$$

Therefore, the present treatment is based on the standard Born–Markov approximation, which combines the assumptions of weak system–reservoir coupling and a memoryless reservoir. This approximation is widely employed in quantum optics for the description of open quantum systems coupled to broadband environments. In quantum optics, a squeezed vacuum state is generated via Eq. (4) leads to Bogoliubov transformation:

$$\hat{c} \to \mu\hat{c} + \nu\hat{d}^{\dagger}, \quad \hat{d} \to \mu\hat{d} + \nu\hat{c}^{\dagger} \tag{35}$$

where $\mu = \cosh r$ and $\nu = e^{i\phi} \sinh r$ for:

$$|\mu_k|^2 - |\nu_k|^2 = 1 \tag{36}$$

From this transformation, one obtains the reservoir averages. Assuming the reservoir parameters vary slowly compared to the system's relaxation rates, the system operates within the adiabatic regime and follows an instantaneous steady state.

$$\langle \hat{c}_k^{\dagger}\hat{c}_{k'} \rangle = N\delta_{kk'}, \quad \langle \hat{c}_k\hat{c}_{k'}^{\dagger} \rangle = (N+1)\delta_{kk'}, \quad \langle \hat{c}_k\hat{c}_{k'} \rangle = M\delta_{k,-k'} \tag{37}$$

For $N = \sinh^2 r$ is mean photon number and $M = |M|e^{i\phi} = \sinh r \cosh r e^{i\phi}$ is squeezing correlation with quantities satisfy the relation $|M|^2 \leq N(N+1)$, ensuring physical consistency with r is squeezing strength and ϕ is squeezing phase. We have the operator identity $\sigma_{13} = \sigma_{12}\sigma_{23}$. Therefore, the coherence σ_{13} can be generated indirectly through the cascade transitions $|3\rangle \leftrightarrow |2\rangle \leftrightarrow |1\rangle$. Moreover, the presence of a squeezed vacuum reservoir introduces phase-sensitive correlations between the two transitions, leading to effective two-photon processes that couple the states $|3\rangle$ and $|1\rangle$. As a result, coherence between these states can be established through correlated emission and absorption processes mediated by the intermediate level $|2\rangle$. Using the reservoir averages given in Eq. (37), it follows immediately that

$$\langle \hat{H}_{AR}(t) \rangle_R = 0. \tag{38}$$

Substituting Eq. (38) into Eq. (29), the equation of motion for the reduced density operator reduces to

$$\begin{aligned} \frac{d\hat{\rho}(t)}{dt} = &\int_0^t \mathrm{Tr}_R\Big(\hat{H}_{AR}(t)\hat{\rho}(t')\hat{H}_{AR}(t')\Big)dt' + \int_0^t \mathrm{Tr}_R\Big(\hat{H}_{AR}(t')\hat{\rho}(t')\hat{H}_{AR}(t)\Big)dt' \\ &- \int_0^t \Big\langle \hat{H}_{AR}(t)\hat{H}_{AR}(t') \Big\rangle_R \hat{\rho}(t')dt' - \int_0^t \hat{\rho}(t') \Big\langle \hat{H}_{AR}(t')\hat{H}_{AR}(t) \Big\rangle_R dt'. \end{aligned} \tag{39}$$

Employing the interaction Hamiltonian Eq. (5), the squeezed-reservoir correlation functions Eq. (37), and the cyclic property of the trace operator, one obtains

$$\begin{aligned}\mathrm{Tr}_R\Big(\hat{H}_{AR}(t)\hat{\rho}(t')\hat{H}_{AR}(t')\Big) &= h_1\hat{\sigma}_{21}\hat{\rho}(t')\hat{\sigma}_{12} + h_1\hat{\sigma}_{32}\hat{\rho}(t')\hat{\sigma}_{23} + h_2\hat{\sigma}_{12}\hat{\rho}(t')\hat{\sigma}_{21} + h_2\hat{\sigma}_{23}\hat{\rho}(t')\hat{\sigma}_{32} \\ &\quad - h_3\hat{\sigma}_{32}\hat{\rho}(t')\hat{\sigma}_{12} - h_3\hat{\sigma}_{21}\hat{\rho}(t')\hat{\sigma}_{32} - h_3\hat{\sigma}_{12}\hat{\rho}(t')\hat{\sigma}_{23} - h_3\hat{\sigma}_{23}\hat{\rho}(t')\hat{\sigma}_{21}. \end{aligned} \tag{40}$$

Similarly,

$$\begin{aligned}\Big\langle \hat{H}_{AR}(t)\hat{H}_{AR}(t')\Big\rangle_R &= h_1\hat{\sigma}_{12}\hat{\sigma}_{21} + h_1\hat{\sigma}_{23}\hat{\sigma}_{32} + h_2\hat{\sigma}_{21}\hat{\sigma}_{12} + h_2\hat{\sigma}_{32}\hat{\sigma}_{23} \\ &\quad - h_3\hat{\sigma}_{12}\hat{\sigma}_{23} - h_3\hat{\sigma}_{12}\hat{\sigma}_{32} - h_3\hat{\sigma}_{23}\hat{\sigma}_{12} - h_3\hat{\sigma}_{32}\hat{\sigma}_{12}. \end{aligned} \tag{41}$$

The coefficients h_1, h_2, and h_3 are defined as

$$h_1 = \sum_{k,k'} \lambda_k\lambda_{k'}\langle \hat{c}_k\hat{c}^{\dagger}_{k'}\rangle\, e^{i(\omega_0-\omega_k)t - i(\omega_0-\omega_{k'})t'}, \tag{42}$$

or equivalently by replacing $\langle \hat{c}_k\hat{c}^{\dagger}_{k'}\rangle$ with $\langle \hat{d}_k\hat{d}^{\dagger}_{k'}\rangle$,

$$h_2 = \sum_{k,k'} \lambda_k\lambda_{k'}\langle \hat{c}^{\dagger}_{k'}\hat{c}_k\rangle\, e^{-i(\omega_0-\omega_k)t + i(\omega_0-\omega_{k'})t'}, \tag{43}$$

or equivalently by replacing $\langle \hat{c}^{\dagger}_{k'}\hat{c}_k\rangle$ with $\langle \hat{d}^{\dagger}_{k'}\hat{d}_k\rangle$,

$$h_3 = \sum_{k,k'} \lambda_k\lambda_{k'}\langle \hat{d}_{k'}\hat{c}_k\rangle\, e^{i(\omega_0-\omega_k)t + i(\omega_0-\omega_{k'})t'}, \tag{44}$$

or equivalently by replacing $\langle \hat{d}_{k'}\hat{c}_k\rangle$ with $\langle \hat{d}^{\dagger}_{k'}\hat{c}^{\dagger}_k\rangle$. For the cascade three-level system $|3\rangle \leftrightarrow |2\rangle \leftrightarrow |1\rangle$, the transition frequencies are

$$\omega_{32} = \frac{E_3 - E_2}{\hbar}, \qquad \omega_{21} = \frac{E_2 - E_1}{\hbar}. \tag{45}$$

Under the near-degenerate approximation,

$$|\omega_1 - \omega_2| \ll \gamma, \kappa, \tag{46}$$

the two transitions become spectrally indistinguishable within the linewidth of the system, allowing one to set

$$\omega_1 \simeq \omega_2, \qquad \omega_0 = \frac{\omega_1 + \omega_2}{2}. \tag{47}$$

The near-degenerate approximation $|\omega_1 - \omega_2| \ll \gamma, \kappa$ is fundamental to preserving the reservoir-induced coherence in our system. In realistic physical implementations, this regime can be achieved using closely spaced Zeeman sublevels or engineered artificial atoms, such as superconducting qubits or tunable semiconductor quantum dots. If this approximation is lifted ($\Delta\omega \gg \gamma$), the rapidly oscillating phase terms $e^{\pm i\Delta\omega t}$ appearing in the cross-dissipative coefficients would average to zero under the secular approximation. Consequently, the phase-sensitive terms proportional to M in the resulting master equation would vanish. Physically, this implies that a highly non-degenerate cascade system cannot support reservoir-mediated two-photon correlations, causing the squeezed reservoir to effectively act as a standard thermal bath governed solely by N, thereby extinguishing the intermodal squeezing and anomalous photon statistics[17],[18]. Using Eq. (37), Eq. (43) becomes

$$h_2 = N\sum_k \lambda_k^2 e^{i(\omega_0-\omega_k)(t-t')}. \tag{48}$$

Assuming a quasi-continuous distribution of reservoir modes, the summation may be replaced by an integration,

$$h_2 = N\int_0^{\infty} g(\omega)\lambda^2(\omega)e^{i(\omega_0-\omega)(t-t')}d\omega, \tag{49}$$

where $g(\omega)$ denotes the density of reservoir modes and $g(\omega)$ and $\lambda(\omega)$ vary negligibly around ω_0, allowing the replacements

$$g(\omega) \simeq g(\omega_0), \qquad \lambda(\omega) \simeq \lambda(\omega_0), \tag{50}$$

and extending the lower integration limit to $-\infty$. Equation (49) then becomes

$$h_2 = Ng(\omega_0)\lambda^2(\omega_0) \int_{-\infty}^{\infty} e^{i(\omega_0-\omega)(t-t')} d\omega. \tag{51}$$

Evaluating the integral yields

$$h_2 = N\gamma\delta(t-t'), \tag{52}$$

where

$$\gamma = 2\pi g(\omega_0)\lambda^2(\omega_0) \tag{53}$$

is the spontaneous-emission decay rate. The appearance of the delta function in Eq. (52) demonstrates explicitly that the reservoir correlations are memoryless,

$$\langle \hat{R}(t)\hat{R}(t')\rangle \propto \delta(t-t'), \tag{54}$$

which is the defining feature of the Markov approximation. Hence, Eqs. (52)–(56) establish that the present derivation is based on the standard Born–Markov treatment of a broadband squeezed reservoir. Proceeding in the same manner, one obtains

$$h_1 = (N+1)\gamma\delta(t-t'), \tag{55}$$

and

$$h_3 = -M\gamma\delta(t-t'). \tag{56}$$

Substituting Eqs. (40), (41), (52), (55), and (56) into Eq. (39), and using the identity

$$\int_0^t f(t')\delta(t-t')dt' = f(t), \tag{57}$$

one obtains the Lindblad-type master equation

$$\begin{aligned}\frac{d\hat{\rho}}{dt} &= \gamma(N+1)\left[\mathcal{D}[\hat{\sigma}_{12}] + \mathcal{D}[\hat{\sigma}_{23}]\right]\hat{\rho} + \gamma N\left[\mathcal{D}[\hat{\sigma}_{12}^{\dagger}] + \mathcal{D}[\hat{\sigma}_{23}^{\dagger}]\right]\hat{\rho} \\ &\quad + \gamma M\left[\mathcal{D}[\hat{\sigma}_{23},\hat{\sigma}_{12}] + \mathcal{D}[\hat{\sigma}_{23}^{\dagger},\hat{\sigma}_{12}^{\dagger}] + \mathcal{D}[\hat{\sigma}_{12},\hat{\sigma}_{23}] + \mathcal{D}[\hat{\sigma}_{12}^{\dagger},\hat{\sigma}_{23}^{\dagger}]\right]\hat{\rho}.\end{aligned} \tag{58}$$

For $\phi = 0$, and the delta-correlated coefficients h_1, h_2, and h_3 ensure that the resulting master equation is local in time. Such a time-local form is valid only under the combined Born and Markov approximations together with the broadband squeezing condition

$$\Delta\omega_s \gg \max(\gamma, \kappa, g). \tag{59}$$

Equation (58) therefore represents the Born–Markov master equation describing the interaction of a cascade three-level atom with a broadband two-mode squeezed vacuum reservoir. The master equation in the standard Gorini–Kossakowski–Sudarshan–Lindblad (GKSL) form, including the phase-sensitive contributions of a squeezed vacuum reservoir, can be written as

$$\frac{d\hat{\rho}}{dt} = -\frac{i}{\hbar}[\hat{H},\hat{\rho}] + \gamma(N+1)\mathcal{D}[\hat{a}]\hat{\rho} + \gamma N\mathcal{D}[\hat{a}^{\dagger}]\hat{\rho} - \gamma M\mathcal{D}_s[\hat{a}]\hat{\rho} - \gamma M^*\mathcal{D}_s[\hat{a}^{\dagger}]\hat{\rho}, \tag{60}$$

where the standard and squeezing dissipators are defined as

$$\mathcal{D}[\hat{O}]\hat{\rho} = \hat{O}\hat{\rho}\hat{O}^{\dagger} - \frac{1}{2}\left\{\hat{O}^{\dagger}\hat{O},\hat{\rho}\right\}, \tag{61}$$

and

$$\mathcal{D}_s[\hat{O}]\hat{\rho} = \hat{O}\hat{\rho}\hat{O} - \frac{1}{2}\left\{\hat{O}\hat{O}, \hat{\rho}\right\}. \tag{62}$$

The parameters N and M denote the mean photon number and two-photon correlation of the squeezed reservoir, respectively, and satisfy $|M|^2 \leq N(N+1)$, which guarantees complete positivity of the density operator. The cross-dissipative terms proportional to $M\gamma$ originate from the phase-sensitive correlations of the squeezed vacuum reservoir. These terms dynamically couple different atomic transitions, such as σ_{12} and σ_{23}, through reservoir-mediated two-photon processes. Importantly, this coupling does not violate the orthogonality of the atomic states. The condition

$$\langle i|j\rangle = \delta_{ij} \tag{63}$$

remains preserved, since the cross terms affect only dynamical correlations between transitions rather than the atomic states themselves. Physically, these terms describe correlated emission and absorption processes involving transitions that share a common intermediate level. Such effects are analogous to interference between decay channels and are well known in systems coupled to squeezed or correlated reservoirs. Therefore, the cross-dissipative terms represent reservoir-induced coherence between transitions and are fully consistent with quantum mechanics. According to the assumptions of quantum Langevin theory, input-output theory, and the Markov approximation,

$$\langle \hat{A}(t')\hat{F}(t)\rangle = 0, \qquad t' < t. \tag{64}$$

Here, $\hat{A}(t')$ is an arbitrary operator associated with the system (e.g., an atom or a cavity), and $\hat{F}(t)$ is a reservoir noise operator. The condition $t' < t$ indicates that the system operator is evaluated at an earlier time than the reservoir noise operator. This relation states that the future reservoir noise is statistically independent of the past state of the system. It further indicates that the reservoir does not retain any memory of previous events occurring within the cavity. This property is known as the Markov property. For a squeezed vacuum results:

$$\langle \hat{a}_i^\dagger(t)\hat{a}_{\mathrm{i,in}}(t)\rangle = \frac{\sqrt{\kappa}N}{2} = \frac{\sqrt{\kappa}}{2}\sinh^2 r, \tag{65}$$

describes a correlation between the intracavity field $\hat{a}_i$ and the incoming reservoir field $\hat{a}_{\mathrm{i,in}}$. The quantity $\hat{a}_i^\dagger(t)\hat{a}_{\mathrm{i,in}}(t)$ measures how strongly the cavity field is correlated with the field entering from the reservoir. Thus, Eq. (64) expresses the memoryless (Markovian) nature of the reservoir, while Eq. (65) quantifies how the reservoir photon population N feeds fluctuations and correlations into the cavity field through the cavity damping channel κ.

Generating the required broadband two-mode squeezed vacuum can be achieved via continuous-wave spontaneous parametric down-conversion (SPDC) in an optical parametric oscillator (OPO) for optical frequencies, or via Josephson Parametric Amplifiers (JPAs) in the microwave regime. For the cascade three-level medium, while natural atomic cascades (e.g., in ^{85}Rb or ^{133}Cs) are viable candidates, artificial atoms in cavity quantum electrodynamics (cQED) offer a highly tunable and practical alternative. Specifically, superconducting transmon qubits exhibit a natural ladder energy-level structure ($|0\rangle \to |1\rangle \to |2\rangle$) that effectively mimics a cascade atom. By placing the transmon inside a heavily overcoupled 3D microwave cavity, the system naturally satisfies the bad-cavity limit ($\kappa \gg g, \gamma$) required for our adiabatic elimination. The injection of squeezed microwave fields into such highly dissipative cavities has already been demonstrated to actively modify qubit decay channels and coherence, making superconducting circuits an ideal platform for observing the reservoir-induced steady-state photon statistics and quadrature squeezing predicted in this model[19]–[21].

1.2. Atomic Operator Dynamics

Lets define the expectation values of operator products as follows:

$$S_{ijk} = \langle \hat{\sigma}_{ij}\hat{\sigma}_{jk}\hat{a}_k\rangle, \quad S^\dagger_{ijk} = \langle \hat{a}_k^\dagger\hat{\sigma}_{ij}\hat{\sigma}_{jk}^\dagger\rangle, \quad T_{ijk} = \langle \hat{a}_k^\dagger\hat{\sigma}_{jk}^\dagger\hat{\sigma}_{ij}\rangle, \quad T^\dagger_{ijk} = \langle \hat{\sigma}_{jk}\hat{\sigma}_{ij}\hat{a}_k\rangle, \quad U_{ijk} = \langle \hat{\sigma}_{jk}\hat{\sigma}_{ij}\hat{\sigma}_{jk}^\dagger\rangle$$
$$V_{ijk} = \langle \hat{\sigma}_{jk}^\dagger\hat{\sigma}_{ij}\hat{\sigma}_{jk}\rangle, \quad W_{ij} = \langle \hat{\sigma}_{ij}\hat{\sigma}_{kk}\rangle, \quad W^\dagger_{ij} = \langle \hat{\sigma}_{kk}\hat{\sigma}_{ij}\rangle, \quad X_{ijk} = \langle \hat{\sigma}_{jk}^\dagger\hat{\sigma}_{ij}\hat{\sigma}_{kl}^\dagger\rangle, \quad Y_{ijk} = \langle \hat{\sigma}_{jk}\hat{\sigma}_{ij}\hat{\sigma}_{kl}\rangle, \tag{66}$$

where $i, j, k, l \in \{1, 2, 3\}$ and k, l indicate the modes (e.g., $k = 1, 2$ for $\hat{a}_1, \hat{a}_2$). Using these definitions, applying the relation $\frac{d\langle\hat{\sigma}_{ij}\rangle}{dt} = Tr\left(\frac{d\hat{\rho}}{dt}\hat{\sigma}_{ij}\right)$ along with Eq. (58) and the cyclic property of the trace operation, can be rewritten as:

$$\frac{d\langle\hat{\sigma}_{ij}\rangle}{dt} = g\sum_{k=1}^{2}\left(S_{ij2k} - S^\dagger_{ij2k} + T_{ij2k} - T^\dagger_{ij2k}\right) + \frac{(N+1)\gamma}{2}\sum_{k=1}^{2}\left(2U_{ij2k} - W_{ij} - W^\dagger_{ij}\right)$$
$$+\frac{N\gamma}{2}\sum_{k=1}^{2}\left(2V_{ij2k} - W_{ij} - W^\dagger_{ij}\right) + \frac{M\gamma}{2}\left(2X_{ij23} + 2Y_{ij23} - W_{ij} - W^\dagger_{ij}\right) + \frac{M\gamma}{2}\left(2Y_{ij31} + 2X_{ij31} - W_{ij} - W^\dagger_{ij}\right) \tag{67}$$

With the aid of Eq. (67), one can readily establish that

$$\frac{d\langle\hat{\sigma}_{12}\rangle}{dt} = -\frac{1}{2}(2+3N)\gamma\langle\hat{\sigma}_{12}\rangle - \frac{1}{2}M\gamma\langle\hat{\sigma}_{23}\rangle + g\left(\langle\hat{a}_1^\dagger\hat{\sigma}_{22}\rangle - \langle\hat{a}_1^\dagger\hat{\sigma}_{11}\rangle + \langle\hat{\sigma}_{13}\hat{a}_2\rangle\right) \tag{68}$$

$$\frac{d\langle\hat{\sigma}_{23}\rangle}{dt} = -\frac{1}{2}(1+3N)\gamma\langle\hat{\sigma}_{23}\rangle - \frac{1}{2}M\gamma\langle\hat{\sigma}_{21}\rangle + g\left(\langle\hat{a}_2^\dagger\hat{\sigma}_{33}\rangle - \langle\hat{a}_2^\dagger\hat{\sigma}_{22}\rangle - \langle\hat{\sigma}_{13}\hat{a}_1\rangle\right) \tag{69}$$

$$\frac{d\langle\hat{\sigma}_{13}\rangle}{dt} = -\frac{1}{2}(1+2N)\gamma\langle\hat{\sigma}_{13}\rangle + \frac{1}{2}M\gamma(2\langle\hat{\sigma}_{22}\rangle - \langle\hat{\sigma}_{11}\rangle - \langle\hat{\sigma}_{33}\rangle) + g(\langle\hat{a}_1^\dagger\hat{\sigma}_{23}\rangle - \langle\hat{a}_2^\dagger\hat{\sigma}_{12}\rangle) \tag{70}$$

$$\frac{d\langle\hat{\sigma}_{11}\rangle}{dt} = -(1+N)\gamma\langle\hat{\sigma}_{11}\rangle + N\gamma\langle\hat{\sigma}_{22}\rangle - \frac{1}{2}M\gamma(\langle\hat{\sigma}_{13}\rangle + \langle\hat{\sigma}_{31}\rangle) + g(\langle\hat{\sigma}_{21}\hat{a}_1\rangle + \hat{a}_1^\dagger\langle\hat{\sigma}_{21}\rangle), \tag{71}$$

$$\begin{aligned}\frac{d\langle\hat{\sigma}_{22}\rangle}{dt} &= -(1+2N)\gamma\langle\hat{\sigma}_{22}\rangle + (1+N)\gamma\langle\hat{\sigma}_{11}\rangle + N\gamma\langle\hat{\sigma}_{33}\rangle + M\gamma(\langle\hat{\sigma}_{13}\rangle + \langle\hat{\sigma}_{31}\rangle) \\ &\quad + g(\langle\hat{\sigma}_{23}\hat{a}_2\rangle - \langle\hat{a}_1^\dagger\hat{\sigma}_{21}\rangle - \langle\hat{\sigma}_{12}\hat{a}_1\rangle + \langle\hat{a}_2^\dagger\hat{\sigma}_{32}\rangle)\end{aligned} \tag{72}$$

$$\frac{d\langle\hat{\sigma}_{33}\rangle}{dt} = -N\gamma\langle\hat{\sigma}_{33}\rangle + (1+N)\gamma\langle\hat{\sigma}_{22}\rangle - \frac{1}{2}M\gamma(\langle\hat{\sigma}_{13}\rangle - \langle\hat{\sigma}_{31}\rangle) + g(\langle\hat{a}_2^\dagger\hat{\sigma}_{32}\rangle + \langle\hat{\sigma}_{23}\hat{a}_2\rangle) \tag{73}$$

We see that Eqs. (68) - (73) are non linear differential equations and hence it is not possible to obtain the exact time dependent solutions of these equations. We carry out our analysis in the bad-cavity limit in which the atomic variables change slowly compared with the cavity modes. Since the cavity modes reach steady state in relatively short period, we can take the time derivatives of such variables to be zero, while keeping the zero-order atomic and cavity mode variables at time t. In the bad-cavity limit, adiabatic elimination of the cavity mode operators is valid when the cavity decay rate κ is much larger than both the atom–field coupling strength g_i and the atomic decay rate γ, $\kappa \gg g_i$, $\kappa \gg \gamma$. Under this condition, the cavity field evolves on a much faster timescale than the atomic variables, allowing the approximation $\dot{\hat{a}}_i \approx 0$. Consequently, the cavity mode operator can be written as

$$\hat{a}_i \approx -\frac{2g_i}{\kappa}\hat{\sigma}_{ji} + \frac{2}{\kappa}\hat{F}_i(t), \tag{74}$$

showing that the cavity field adiabatically follows the atomic dynamics. This approximation remains valid as long as the effective atom–field interaction strength satisfies $g_i \ll \kappa$, so that the cavity field decays before a significant population can build up. Such conditions are commonly realized in bad-cavity quantum optical systems and are consistent with standard treatments of open quantum systems and quantum Langevin dynamics. In view of this, we have from Eqs. (21) and (22) that

$$\hat{a}_1 \approx -\frac{2g}{\kappa}\hat{\sigma}_{21} + \frac{2}{\kappa}\hat{F}_1(t), \tag{75}$$

and

$$\hat{a}_2 \approx -\frac{2g}{\kappa}\hat{\sigma}_{32} + \frac{2}{\kappa}\hat{F}_2(t). \tag{76}$$

The first terms represent the cavity fields induced by the atomic transitions, while the second terms describe the fluctuations injected by the squeezed reservoir through the noise operators $\hat{F}_1$ and $\hat{F}_2$. We explicitly define our truncation scheme by applying the semi-classical decoupling $\langle\hat{\sigma}_{ij}\hat{F}_k\rangle \approx \langle\hat{\sigma}_{ij}\rangle\langle\hat{F}_k\rangle = 0$. The physical validity of this approximation rests entirely on the strict broadband limit of the squeezed vacuum reservoir ($\Delta\omega_s \gg \kappa, g, \gamma$). In this regime, the reservoir acts as a delta-correlated, memoryless Markovian bath ($\tau_s \to 0$), meaning the atomic operators cannot establish a steady-state correlation with instantaneous noise fluctuations. However, we must note that this truncation fundamentally limits our model in the strong-coupling regime ($g \sim \kappa$) or if the squeezed vacuum possesses a finite bandwidth. Recent investigations into noise-induced dynamics within quantum-dot micropillar lasers have demonstrated that un-truncated stochastic noise correlations can induce significant quantum feedback[22],[23]. Such noise-driven interactions structurally alter the cavity photon statistics, frequently driving the emitted light into super-thermal bunching regimes ($g^{(2)}(0) > 2$). Given the robust, phase-sensitive two-photon correlations inherent

to squeezed-vacuum fluctuations, future models lifting this mean-field truncation to map higher-order quantum feedback will likely reveal even more pronounced transitions between anti-bunching and super-bunching phenomena. For the present work, our analytical boundaries are strictly confined to the weak-coupling, broadband bad-cavity limit where the truncation remains dynamically stable. By substituting Eqs. (75) and (76) into Eqs. (68)- (73) under the bad-cavity limit, and applying the semi-classical approximation to neglect higher-order correlations between the atomic and field operators, we obtain:

$$\frac{d\langle\hat{\sigma}_{12}\rangle}{dt} = -\frac{1}{2}(2+2\eta+3N)\langle\hat{\sigma}_{12}\rangle - \frac{1}{2}M\langle\hat{\sigma}_{23}\rangle, \tag{77}$$

$$\frac{d\langle\hat{\sigma}_{23}\rangle}{dt} = -\frac{1}{2}(1+\eta+3N)\langle\hat{\sigma}_{23}\rangle - \frac{1}{2}M\langle\hat{\sigma}_{21}\rangle, \tag{78}$$

$$\frac{d\langle\hat{\sigma}_{13}\rangle}{dt} = -\frac{1}{2}(1+\eta+2N)\gamma\langle\hat{\sigma}_{13}\rangle + \frac{1}{2}M\gamma(2\langle\hat{\sigma}_{22}\rangle - \langle\hat{\sigma}_{11}\rangle - \langle\hat{\sigma}_{33}\rangle), \tag{79}$$

$$\frac{d\langle\hat{\sigma}_{11}\rangle}{dt} = -(1+\eta+N)\langle\hat{\sigma}_{11}\rangle + N\langle\hat{\sigma}_{22}\rangle - M\langle\hat{\sigma}_{13}\rangle, \tag{80}$$

$$\frac{d\langle\hat{\sigma}_{22}\rangle}{dt} = -(1+\eta+2N)\langle\hat{\sigma}_{22}\rangle + (1+N+\eta)\langle\hat{\sigma}_{11}\rangle + N\langle\hat{\sigma}_{33}\rangle + 2M\langle\hat{\sigma}_{13}\rangle \tag{81}$$

$$\frac{d\langle\hat{\sigma}_{33}\rangle}{dt} = -N\langle\hat{\sigma}_{33}\rangle + (1+\eta+N)\langle\hat{\sigma}_{22}\rangle - M\langle\hat{\sigma}_{13}\rangle. \tag{82}$$

where η serves as the factor of effective cooperativity parameter of the system. It is defined as the ratio of the cavity-enhanced stimulated emission rate to the free-space spontaneous decay rate, given by

$$\eta = \frac{\gamma_3}{\gamma}. \tag{83}$$

This parameter quantifies the dominance of atom-cavity interaction over spontaneous environmental losses and $\gamma_3 = \frac{4g^2}{\kappa}$ being the stimulated emission decay constant due to the atom interacts with the cavity modes and choosing the atomic coherence to be real $\langle\hat{\sigma}_{31}\rangle = \langle\hat{\sigma}_{13}\rangle$. Based on the definition of this decay constant, we infer that an atom in upper or middle level emits a photon due to interaction with cavity modes. We certainly identify the process to be stimulated photon emission. With the aid of Eqs. (77) - (82), the expectation values of the atomic operators at steady state can be expressed as

$$\langle\hat{\sigma}_{12}\rangle = \langle\hat{\sigma}_{23}\rangle = 0, \tag{84}$$

$$\langle\hat{\sigma}_{13}\rangle = \frac{M}{1+\eta+2N}\left(2\langle\hat{\sigma}_{22}\rangle - \langle\hat{\sigma}_{11}\rangle - \langle\hat{\sigma}_{33}\rangle\right), \tag{85}$$

$$(1+\eta+N)\langle\hat{\sigma}_{11}\rangle - N\langle\hat{\sigma}_{22}\rangle + M\langle\hat{\sigma}_{13}\rangle = 0, \tag{86}$$

$$(1+\eta+N)\langle\hat{\sigma}_{11}\rangle - (1+\eta+2N)\langle\hat{\sigma}_{22}\rangle + N\langle\hat{\sigma}_{33}\rangle + 2M\langle\hat{\sigma}_{13}\rangle = 0, \tag{87}$$

$$(1+\eta+N)\langle\hat{\sigma}_{22}\rangle - N\langle\hat{\sigma}_{33}\rangle - M\langle\hat{\sigma}_{13}\rangle = 0. \tag{88}$$

Furthermore, using the normalization condition $\hat{I} = \hat{\sigma}_{11} + \hat{\sigma}_{22} + \hat{\sigma}_{33}$, we can write

$$\langle\hat{\sigma}_{13}\rangle = \frac{3M\langle\hat{\sigma}_{22}\rangle - M}{1+2N+\eta}, \tag{89}$$

$$\langle\hat{\sigma}_{11}\rangle = \frac{M^2 - N(2+N-\eta)\langle\hat{\sigma}_{22}\rangle}{(1+\eta+N)(1+\eta+2N)}, \tag{90}$$

$$\langle\hat{\sigma}_{22}\rangle = \frac{2M^2 - (1+\eta+2N)\left((1+N+\eta)\langle\hat{\sigma}_{11}\rangle + N\langle\hat{\sigma}_{33}\rangle\right)}{6M^2 - (1+\eta+2N)^2}, \tag{91}$$

$$\langle\hat{\sigma}_{33}\rangle = \frac{M^2 + \left((1+\eta+N)(1+\eta+2N) - 3M^2\right)\langle\hat{\sigma}_{22}\rangle}{N(1+\eta+2N)}. \tag{92}$$

Solving simultaneously, we find

$$\langle\hat{\sigma}_{11}\rangle = \frac{N(1+\eta+2N\eta)}{(1+\eta+2N)[(1+\eta)^2+3N\eta]}, \tag{93}$$

$$\langle\hat{\sigma}_{22}\rangle = \frac{N\eta(1+\eta+2N)}{(1+\eta+2N)[(1+\eta)^2+3N\eta]}, \tag{94}$$

$$\langle\hat{\sigma}_{33}\rangle = \frac{(1+\eta+N)(1+\eta+2N\eta)+\eta(1+\eta)(1+\eta+2N)}{(1+\eta+2N)[(1+\eta)^2+3N\eta]}. \tag{95}$$

$$\langle\hat{\sigma}_{13}\rangle = -\frac{M(1+\eta)^2}{(1+\eta+2N)[(1+\eta)^2+3N\eta]}, \tag{96}$$

1.3. Properties of two cavity modes a_1 and a_1

In this section we wish to calculate the mean, the normalized second-order correlation function, and the quadrature variance of cavity mode a_1 and mode a_2 at steady state.

1.3.1. The Mean Photon Number

The mean photon number is used to understand the intensity, state, interaction strength, and thermodynamic behavior of cavity light because it is a core quantity in quantum optics, quantum information, and quantum technologies. In case one seeks to reproduce the result of the experiment, it is the statistical mean of the measured values that perhaps can be calculated. The mean photon number for cavity mode a_1 and mode a_2 are defined by

$$\bar{n}_{a_1} = \langle\hat{a_1}^\dagger\hat{a_1}\rangle_{ss}, \tag{97}$$

$$\bar{n}_{a_2} = \langle\hat{a_2}^\dagger\hat{a_2}\rangle_{ss}. \tag{98}$$

Taking into account Eqs. (75) and (76) along with the adjoins of Eqs. (75) and (76), we see that

$$\bar{n}_{a_1} = \frac{\gamma_3}{\kappa}\langle\hat{\sigma}_{11}\rangle + \frac{4N}{\kappa}, \tag{99}$$

and

$$\bar{n}_{a_2} = \frac{\gamma_3}{\kappa}\langle\hat{\sigma}_{22}\rangle + \frac{4N}{\kappa}. \tag{100}$$

Applying Eqs. (93) and (94), we find

$$\bar{n}_{a_1} = \frac{N\left[\gamma_3(1+\eta+2N\eta)+4(1+2N+\eta)\left((1+\eta)^2+3N\eta\right)\right]}{\kappa(1+2N+\eta)\left[(1+\eta)^2+3N\eta\right]}, \tag{101}$$

and

$$\bar{n}_{a_2} = \frac{N\left[\gamma_3\eta(1+2N+\eta)+4(1+2N+\eta)\left((1+\eta)^2+3N\eta\right)\right]}{\kappa(1+2N+\eta)\left[(1+\eta)^2+3N\eta\right]}. \tag{102}$$

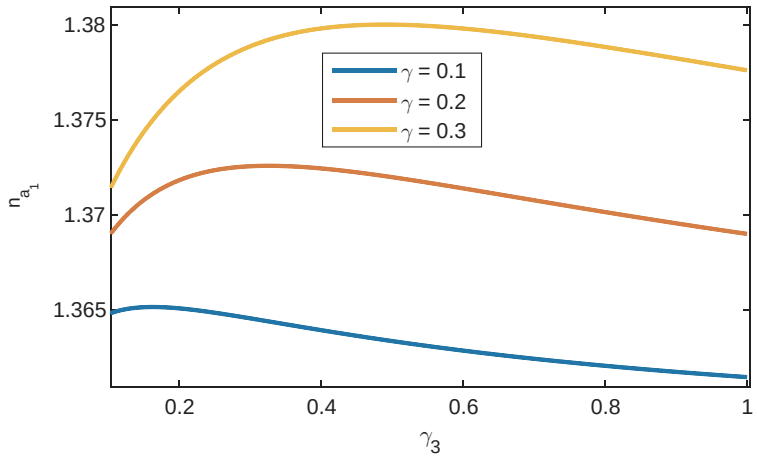


FIG. 2: Plots of mean photon number for mode a_1 [*Eqs.* (101)] versus γ_3 for $\kappa = 0.8$, $r = 0.5$, and for different values of γ.

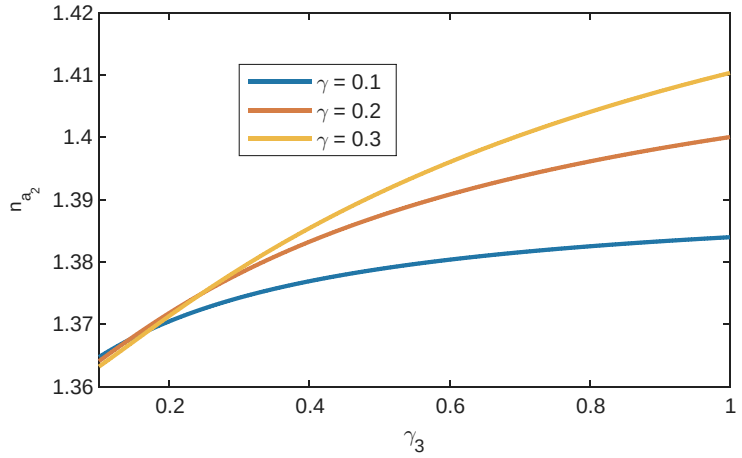


FIG. 3: Plots of mean photon number for mode a_2 [Eq. (102)] versus γ_3 for $\kappa = 0.8$, $r = 0.5$, and for different values of γ.

Figures 2–5 present the steady-state mean photon numbers, $\bar{n}_{a_1}$ and $\bar{n}_{a_2}$, as functions of the stimulated-emission decay constant γ_3 for different values of the squeezing parameter r and the spontaneous decay rate γ. Figures 4 and 5 show that both $\bar{n}_{a_1}$ and $\bar{n}_{a_2}$ increase with increasing values of the squeezing parameter r. The corresponding curves remain nearly constant with respect to γ_3, indicating that the squeezed-vacuum reservoir dominates the photon statistics in this regime. The increase in photon number with r arises because the two-mode squeezed-vacuum reservoir injects correlated photon pairs into the cavity. As discussed in[24], the squeezed reservoir enhances both the mean photon number and quantum correlations by reducing vacuum fluctuations and amplifying coherent emission processes. Consequently, the behavior observed in Figs. 4 and 5 reflects reservoir-induced amplification, suppression of quantum noise, and enhancement of correlated photon generation. This weak dependence on γ_3 indicates that, in the presence of strong squeezing, the atom–reservoir interaction dominates over the atom–cavity dynamics.

In contrast, Figs. 2 and 3 exhibit a strong dependence on γ_3 when the squeezing parameter is held fixed. The mean photon number $\bar{n}_{a_1}$ displays a non-monotonic behavior: it initially increases with γ_3, reaches a maximum value, and then decreases. This behavior results from the competition among several physical mechanisms, including enhanced stimulated emission associated with increasing γ_3, cavity losses characterized by the cavity damping rate κ, atomic population depletion, and energy transfer to mode a_2. The resulting peak structure is a characteristic feature of nonlinear quantum optical systems and provides clear evidence of gain–loss competition. The mean photon number $\bar{n}_{a_2}$, on the other hand, increases monotonically with γ_3, indicating the presence of a gain-dominated regime. This behavior originates from the cascade transition ($|2\rangle \rightarrow |3\rangle$), which is continuously fed by photons generated through the upper transition. According to [Eq. (102)], the dominant contribution scales as $\gamma_3\eta \propto \gamma_3^2/\gamma$, leading to strong nonlinear amplification and a continuous increase in the photon population of mode a_2.

A comparison between Figs. 4–5 and Figs. 2–3 reveals two distinct operating regimes. In the squeezing-dominated regime, the photon numbers increase with the squeezing parameter r and remain nearly independent of γ_3. In the cavity-dynamics-dominated regime, however, the photon numbers depend strongly on γ_3 and exhibit pronounced nonlinear behavior. These observations demonstrate that the squeezed-vacuum reservoir can effectively override

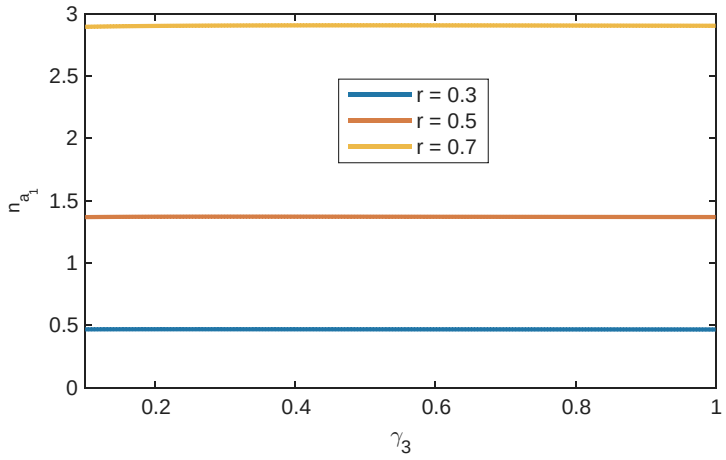


FIG. 4: Plots of mean photon number for mode a_1 [Eq. (101)] versus γ_3 for $\kappa = 0.8$, $\gamma = 0.2$, and for different values of r.

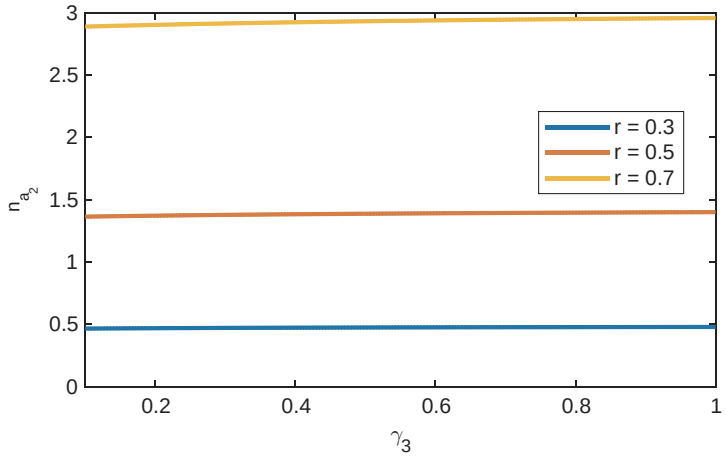


FIG. 5: Plots of mean photon number for mode a_2 [Eq. (102)] versus γ_3 for $\kappa = 0.8$, $\gamma = 0.2$, and for different values of r.

the intrinsic cavity dynamics and control the statistical properties of the generated radiation. The atom–cavity interaction, governed by γ_3, determines the rate of stimulated emission and photon generation. Increasing γ_3 strengthens the coupling and modifies the energy distribution between the two cavity modes. In contrast, the atom–reservoir interaction, mediated by the squeezed-vacuum field, introduces quantum correlations and suppresses fluctuations. As reported in[24], the squeezed reservoir significantly enhances squeezing and entanglement while simultaneously exerting a strong influence on the photon statistics.

The results reveal several notable features, including the existence of distinct regimes controlled by the squeezing parameter r and the stimulated-emission decay constant γ_3, asymmetric photon dynamics between the two modes, non-monotonic behavior in mode a_1 and monotonic amplification in mode a_2, substantial enhancement of nonclassical properties by the squeezed-vacuum reservoir, and the generation of highly correlated and entangled two-mode radiation. These findings highlight the potential of the system as a controllable source of nonclassical light for applications in quantum communication, quantum metrology, and continuous-variable quantum information processing.

The mean photon number sum and difference of mode a_1 and cavity mode a_2 defined by

$$\bar{n}_{\pm} = \bar{n}_{a_1} \pm \bar{n}_{a_2}. \tag{103}$$

Taking into account Eqs. (101) and (102), we have

$$\bar{n}_{\pm} = \frac{N}{\kappa} \frac{\gamma_3 \Big[(1+\eta)(1\pm\eta) + 2N\eta(1\pm 1)\Big] + 4(1\pm 1)(1+2N+\eta)\Big[(1+\eta)^2 + 3N\eta\Big]}{(1+2N+\eta)\Big[(1+\eta)^2 + 3N\eta\Big]}. \tag{104}$$

Figs. 6–9 present the behavior of the mean photon number difference, $\bar{n}_-$, and the mean photon number sum, $\bar{n}_+$, as functions of the stimulated-emission decay constant γ_3 for different values of the spontaneous decay rate γ and the squeezing parameter r.

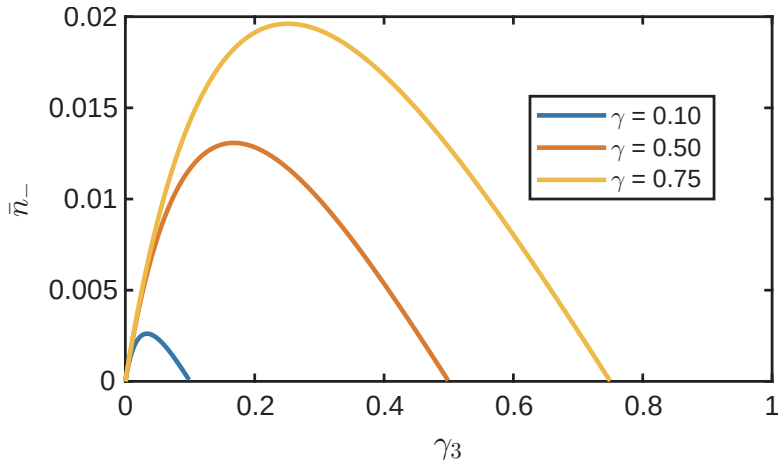


FIG. 6: Plots of mean photon number difference [Eq. (104)] versus γ_3 for $\kappa = 0.8$, different value of γ and $r = 0.5$.

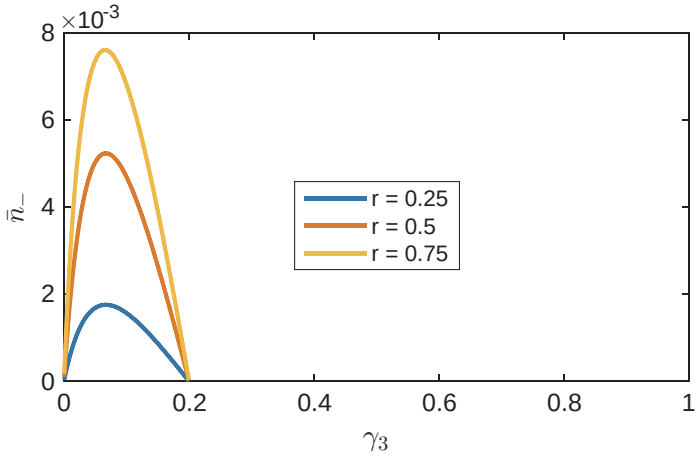


FIG. 7: Plots of mean photon number difference [Eq. (104)] versus γ_3 for $\kappa = 0.8$, $\gamma = 0.2$ and different value of r.

Figs. 6 and 7 demonstrate that the steady-state mean photon-number difference exhibits a pronounced non-monotonic dependence on the stimulated-emission decay constant. Initially, increasing γ_3 enhances cavity-assisted stimulated emission, thereby increasing the photon-number imbalance. However, as the effective cooperativity $\eta = \frac{\gamma_3}{\gamma}$ approaches unity, cooperative atom-cavity interactions and saturation effects suppress the imbalance, leading to $\bar{n}_- = 0$ at $\eta = 1$. Reducing the spontaneous decay rate increases the maximum photon-number difference by weakening environmental dissipation, whereas increasing the squeezing parameter amplifies the imbalance through enhanced two-photon correlations of the squeezed-vacuum reservoir. With the reservoir phase fixed at $\phi = 0$, constructive phase-sensitive interference maximizes correlated photon transfer into the cavity modes. These results reveal that the photon-number difference is governed by the interplay between coherent cavity-enhanced stimulated emission, irreversible spontaneous decay, and phase-sensitive quantum correlations of the squeezed reservoir, providing a clear signature of cooperativity-controlled nonclassical photon dynamics in an open two-mode cavity-QED system. This interpretation is consistent with Eq. (104), the definition of cooperativity in Eq. (83), the Purcell-enhanced stimulated-emission rate $\gamma_3 = \frac{4g^2}{\kappa}$, and the fundamental balance between coherent interaction and dissipative quantum noise in open quantum optical systems.

Figs. 8 and 9 demonstrate that the steady-state mean photon-number sum increases monotonically with the cavity-enhanced stimulated-emission rate and is strongly amplified by the squeezing strength of the two-mode vacuum reservoir. Unlike the photon-number difference, the total photon population remains positive because Eq. (104) contains only constructive contributions for the plus mode. Increasing the atom-cavity coupling enhances Purcell-enhanced photon generation, while increasing the squeezing parameter amplifies phase-sensitive two-photon correlations. For $\phi = 0$, constructive interference maximizes the transfer of quantum correlations from the reservoir into the cavity modes. Remarkably, substantial intracavity photon populations are generated without external pumping, even in the bad-cavity limit. These findings reveal that reservoir-engineered quantum fluctuations, combined with cavity-enhanced spontaneous emission, provide an efficient mechanism for producing nonclassical light in highly dissipative open quantum systems. This pump-free photon generation constitutes a distinctive feature of the present two-mode

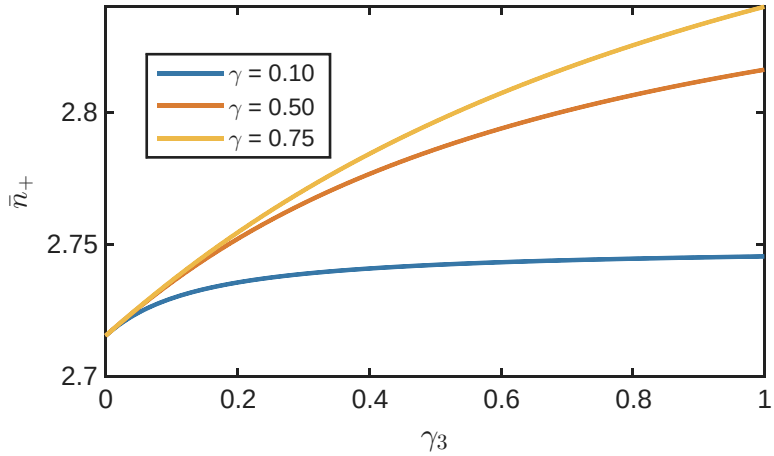


FIG. 8: Plots of mean photon number plus [Eq. (104)] versus γ_3 for $\kappa = 0.8$, different value of γ and $r = 0.5$.

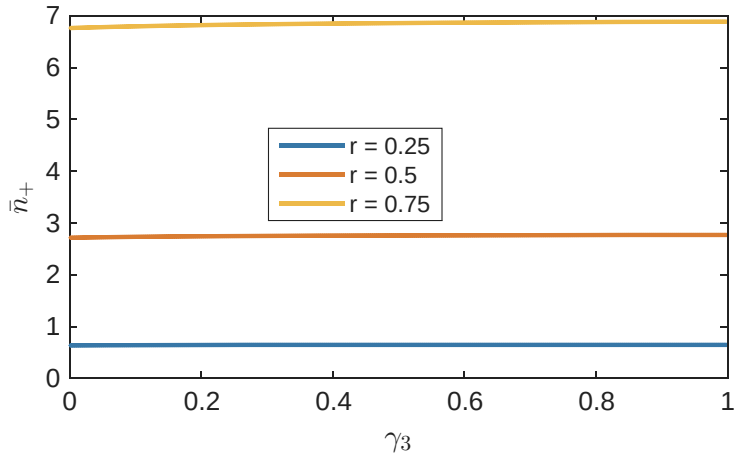


FIG. 9: Plots of mean photon number plus [Eq. (104)] versus γ_3 for $\kappa = 0.8$, $\gamma = 0.2$ and different value of r.

cavity-QED system and offers a new route toward quantum light sources based solely on engineered dissipation and cooperative quantum dynamics.

The results reveal several notable features, including simultaneous control of the total photon number and intermodal imbalance, a strong dependence of photon statistics on the squeezing parameter r, distinct roles of γ_3 and r in regulating intensity and correlations, and the generation of highly correlated nonclassical two-mode radiation. These findings demonstrate the potential of the system as an efficient source of controllable quantum light for applications in quantum communication, quantum metrology, and continuous-variable quantum information processing.

1.3.2. Normalized Second Order-Correction Function

To characterize the quantum nature of light by analyzing its photon statistics let us calculate the second-order correction function at steady state. The normalized second-order correlation function for mode a_1 and mode a_2 are defined by

$$g_{a_1}{}^{(2)}(0) = \frac{\langle \hat{a_1}^{\dagger 2} \hat{a_1}^2 \rangle}{\langle \hat{a_1}^{\dagger} \hat{a_1} \rangle^2}, \tag{105}$$

$$g_{a_2}{}^{(2)}(0) = \frac{\langle \hat{a_2}^{\dagger 2} \hat{a_2}^2 \rangle}{\langle \hat{a_2}^{\dagger} \hat{a_2} \rangle^2} \tag{106}$$

The photons will exhibit super-Poissonian, Poissonian, and sub-Poissonian statistical properties if the normalized second-order correlation function of their cavity mode has value $g_i^{(2)}(0) > 1$, $g_i^{(2)}(0) = 1$, and $g_i^{(2)}(0) < 1$, respectively. With the aid of Eqs. (75), (76), (93), (94), and (95), we have

$$[\hat{a_1}, \hat{a_1}^{\dagger}] = \frac{\gamma_3}{\kappa} (\hat{\sigma}_{22} - \hat{\sigma}_{11}) + \frac{4}{\kappa}, \tag{107}$$

$$[\hat{a_2}, \hat{a_2}^\dagger] = \frac{\gamma_3}{\kappa}\left(\hat{\sigma}_{33} - \hat{\sigma}_{22}\right) + \frac{4}{\kappa}. \tag{108}$$

Using Eqs. (105) and (106), Eqs. (107) and (108) can be written in the form

$$g_{a_1}{}^{(2)}(0) = 1 + \frac{\Delta n_{a_1}^2 - \langle \hat{a_1}^\dagger[\hat{a_1}, \hat{a_1}^\dagger]\hat{a_1}\rangle}{\bar{n}_{a_1}^2}, \tag{109}$$

$$g_{a_2}{}^{(2)}(0) = 1 + \frac{\Delta n_{a_2}^2 - \langle \hat{a_2}^\dagger[\hat{a_2}, \hat{a_2}^\dagger]\hat{a_2}\rangle}{\bar{n}_{a_2}^2}. \tag{110}$$

The photon number variance of mode a_1 and mode a_2 are defined as

$$\Delta n_{a_1}^2 = \langle(\hat{a_1}^\dagger\hat{a_1})^2\rangle - \langle\hat{a_1}^\dagger\hat{a_1}\rangle^2, \tag{111}$$

$$\Delta n_{a_2}^2 = \langle(\hat{a_2}^\dagger\hat{a_2})^2\rangle - \langle\hat{a_2}^\dagger\hat{a_2}\rangle^2. \tag{112}$$

Applying the adiabatic elimination results from Eqs. (75) and (76) alongside the steady-state populations in Eqs. (93) and (94), the photon number variances can be written in terms of atomic variables as

$$\Delta n_{a_1}^2 = \frac{\gamma_3^2}{\kappa^2}\langle\hat{\sigma}_{11}\rangle\left(1 - \langle\hat{\sigma}_{11}\rangle\right) + \frac{16N}{\kappa^3} + \frac{16N(N+1)}{\kappa^2}, \tag{113}$$

$$\Delta n_{a_2}^2 = \frac{\gamma_3^2}{\kappa^2}\langle\hat{\sigma}_{22}\rangle\left(1 - \langle\hat{\sigma}_{22}\rangle\right) + \frac{16N}{\kappa^3} + \frac{16N(N+1)}{\kappa^2}. \tag{114}$$

Furthermore, using Eqs. (75), (76), (107) and (108), we can write as

$$\left\langle \hat{a_1}^\dagger[\hat{a}_1, \hat{a}_1^\dagger]\hat{a}_1 \right\rangle = \frac{1}{\kappa^2}\left[(\gamma_3^2 + 4\gamma_3)\langle\hat{\sigma}_{11}\rangle + 4\gamma_3 N\langle\hat{\sigma}_{22} - \hat{\sigma}_{11}\rangle + 16N\right]. \tag{115}$$

$$\langle\hat{a_2}^\dagger[\hat{a_2}, \hat{a_2}^\dagger]\hat{a_2}\rangle = \frac{1}{\kappa^2}\left[(\gamma_3^2 + 4\gamma_3)\langle\hat{\sigma}_{22}\rangle + 4\gamma_3 N\langle\hat{\sigma}_{33} - \hat{\sigma}_{22}\rangle + 16N\right]. \tag{116}$$

Employing Eqs. (113), (114), (115), and (116) in Eq. (109) and (110), we have

$$g_{a_1}^{(2)}(0) = \frac{4\left[8N^2 + \frac{4N}{\kappa} + \gamma_3(3N-1)\langle\hat{\sigma}_{11}\rangle - \gamma_3 N\langle\hat{\sigma}_{22}\rangle\right]}{\left(\gamma_3\langle\hat{\sigma}_{11}\rangle + 4N\right)^2}, \tag{117}$$

$$g_{a_2}^{(2)}(0) = \frac{4\left[8N^2 + \frac{4N}{\kappa} + \gamma_3(3N-1)\langle\hat{\sigma}_{22}\rangle - \gamma_3 N\langle\hat{\sigma}_{33}\rangle\right]}{\left(\gamma_3\langle\hat{\sigma}_{22}\rangle + 4N\right)^2}, \tag{118}$$

so that substitution on account of Eqs. (93) and (94) yields

$$g_{a_1}^{(2)}(0) = \frac{4D\Big[4D(2N\kappa+1) + \kappa\gamma_3(3N - 1 - \eta + 4N^2\eta - N\eta^2)\Big]}{N\kappa\Big[\gamma_3(1+\eta+2N\eta) + 4D\Big]^2}, \tag{119}$$

where $D = (1+\eta+2N)\Big[(1+\eta)^2 + 3N\eta\Big]$.

$$g_{a_2}^{(2)}(0) = \frac{4D\Big[4D(2N\kappa+1) + \kappa\gamma_3\big(4N^2\eta - N(1+4\eta+\eta^2) - (1+4\eta+4\eta^2+\eta^3)\big)\Big]}{N\kappa\Big[\gamma_3\eta(1+\eta+2N) + 4D\Big]^2} \tag{120}$$

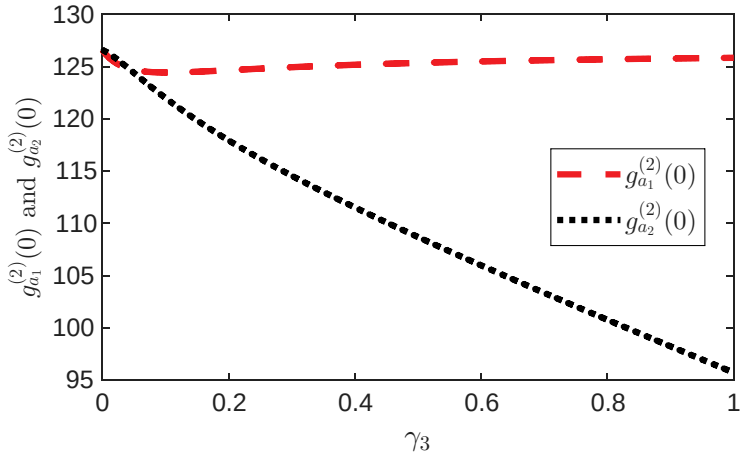


FIG. 10: Plots of the normalized second-order correlation function for mode a_1, $g^{(2)}_{a_1}(0)$ [*Eq.* (119)], and mode a_2, $g^{(2)}_{a_2}(0)$, [Eq. (120)] versus γ_3 for $r = 0.1$, $\gamma = 0.1$, and $\kappa = 0.8$.

Eqs. (119) and (120) represents normalized second-order correlation function for mode a_1 and mode a_2, respectively. The normalized second-order correlation functions, Fig. 10, exhibit a nontrivial dependence on the stimulated-emission decay constant, γ_3, revealing the competition between the two-mode squeezed-vacuum reservoir and the cascade three-level atomic medium. The observed behavior can be understood through three distinct dynamical regimes. For weak atom-cavity coupling, the cavity dynamics are dominated by the squeezed-vacuum reservoir. In this regime, the reservoir injects strongly correlated photon pairs into the cavity modes, leading to large intensity fluctuations and pronounced photon bunching. Consequently, both $g^{(2)}_{a_1}(0)$ and $g^{(2)}_{a_2}(0)$ attain values significantly greater than unity, indicating strongly super-Poissonian photon statistics. This behavior is characteristic of squeezed-vacuum fields, which enhance pairwise photon correlations and generate thermal-like photon-number fluctuations. As γ_3 increases, the influence of the active atomic medium becomes increasingly significant, causing both correlation functions to decrease. This reduction originates from the sequential-emission nature of the cascade transition. Since an atom must emit through the upper transition before the lower transition can occur, the photon-generation process becomes temporally ordered. Such ordering suppresses the random photon clustering induced by the squeezed reservoir and regulates the emission dynamics. As a result, the system demonstrates a pronounced suppression of the extreme super-Poissonian bunching initially induced by the squeezed reservoir. While the correlation functions remain strictly super-Poissonian ($g^{(2)}(0) \gg 1$) within this parameter regime due to the massive injection of highly correlated photon pairs, the sequential nature of the cascade emission acts as an intrinsic regulating mechanism. This is particularly evident in mode a_2, where the temporal ordering of the atomic decay continuously drives the photon statistics downward, effectively mitigating the severe intensity fluctuations characteristic of the squeezed bath this align with[25]. For sufficiently large values of γ_3, atomic saturation and spontaneous-emission processes introduce additional incoherent noise into the cavity modes. These fluctuations partially destroy the antibunching established at intermediate coupling strengths, causing the correlation functions to increase gradually toward asymptotic values associated with a partially thermalized field.

A comparison of the two modes reveals a clear quantum-optical asymmetry; the upper-transition mode, a_1, generally retains larger values of $g^{(2)}(0)$, reflecting stronger residual photon bunching. In contrast, the lower-transition mode, a_2, exhibits significantly deeper antibunching because its emission is conditioned on the prior emission of mode a_1. This intrinsic temporal memory effectively suppresses intensity fluctuations, producing the pronounced minimum observed in $g^{(2)}_{a_2}(0)$. The key novelty of this work is the demonstration that a cascade three-level atom coupled to a squeezed-vacuum reservoir can simultaneously sustain continuous-variable quantum correlations and discrete-variable photon antibunching. While squeezed reservoirs are known to generate squeezing, entanglement, and steering, they typically enhance photon bunching. Our results show that the cascade atomic structure acts as an intrinsic photon-regulation mechanism that suppresses reservoir-induced intensity fluctuations. In particular, mode a_2 maintains strong sub-Poissonian statistics even in the presence of a bunching squeezed reservoir ($r = 0.1$). This unique interplay enables the simultaneous generation of squeezing, entanglement, and antibunched light, making the system highly promising for quantum communication and quantum information applications.

1.4. Quadrature Variance

Quantification of the degree of squeezing in practical framework encompasses detailed calculation of moments such as correlations and mean photon number. In continuous-variable quantum optics, the resilience of scalar observables such as the mean photon number $\overline{n}$ and the normalized second-order coherence $g^{(2)}(0)$ against variations in the squeezing phase ϕ fundamentally relies upon the system's amplitude displacement. For a pure squeezed vacuum

state lacking coherent displacement ($\alpha = 0$), these photon statistics remain entirely invariant. This robustness occurs because the phase is mathematically encoded within the complex squeeze factor, $\xi = re^{i\phi}$. Altering ϕ strictly preserves the squeezing magnitude r. Instead, it elegantly rotates the squeezing ellipse in phase space, redistributing quantum noise across orthogonal quadratures without compromising continuous-variable correlations or photon-pair generation rates. Conversely, introducing a non-zero amplitude displacement intentionally shatters this established invariance. Quantum interference between displacement and squeezing amplitudes forces observables like $g^{(2)}(0)$ to display a 2π-periodic dependence on the squeezing phase. This elegant mechanism enables the continuous tuning of photon statistics, seamlessly bridging particle-like anti-bunching and wave-like quantum super-bunching regimes[26]. The squeezing properties of mode a_1 and mode a_2 are described by two quadrature operators defined by

$$\hat{a}_{\pm} = \sqrt{\pm 1}\left(\hat{a_1}^{\dagger} \pm \hat{a_1}\right), \tag{121}$$

$$\hat{b}_{\pm} = \sqrt{\pm 1}\left(\hat{a_2}^{\dagger} \pm \hat{a_2}\right). \tag{122}$$

Thus in the next let calculate the quadrature mode a_1 and mode a_2 using Eq. (75) and Eq. (76).

$$\hat{a}_{+} = -\sqrt{\frac{\gamma_3}{\kappa}}\left(\hat{\sigma}_{21} + \hat{\sigma}_{12}\right) + \frac{2}{\kappa}\left(\hat{F}_1 + \hat{F}_1^{\dagger}\right), \quad \hat{a}_{-} = i\sqrt{\frac{\gamma_3}{\kappa}}\left(\hat{\sigma}_{21} - \hat{\sigma}_{12}\right) + \frac{2i}{\kappa}\left(\hat{F}_1^{\dagger} - \hat{F}_1\right), \tag{123}$$

and

$$\hat{b}_{+} = -\sqrt{\frac{\gamma_3}{\kappa}}\left(\hat{\sigma}_{32} + \hat{\sigma}_{23}\right) + \frac{2}{\kappa}\left(\hat{F}_2 + \hat{F}_2^{\dagger}\right), \quad \hat{b}_{-} = i\sqrt{\frac{\gamma_3}{\kappa}}\left(\hat{\sigma}_{32} - \hat{\sigma}_{23}\right) + \frac{2i}{\kappa}\left(\hat{F}_2^{\dagger} - \hat{F}_2\right). \tag{124}$$

Using the quadrature commutation relations $[\hat{a}_+, \hat{a}_-] = 2i[\hat{a}_1, \hat{a}_1^{\dagger}]$ and $[\hat{b}_+, \hat{b}_-] = 2i[\hat{a}_2, \hat{a}_2^{\dagger}]$, and substituting the operator-valued commutators from Eq. (107) and Eq. (108), it can be readily established that:

$$[\hat{a}_+, \hat{a}_-] = i\frac{2\gamma_3}{\kappa}\left(\hat{\sigma}_{22} - \hat{\sigma}_{11}\right) + \frac{8i}{\kappa}, \tag{125}$$

$$\left[\hat{b}_+, \hat{b}_-\right] = i\frac{2\gamma_3}{\kappa}\left(\hat{\sigma}_{33} - \hat{\sigma}_{22}\right) + \frac{8i}{\kappa}. \tag{126}$$

The uncertainty relation of two physical observations A and B satisfying the commutation relation:

$$\left[\hat{A}, \hat{B}\right] = i\hat{C} \tag{127}$$

is

$$\Delta A^2 \Delta B^2 \geq \frac{1}{4}\left|\langle \hat{C} \rangle\right|^2. \tag{128}$$

In view of this, we can easily establish the uncertainty relations for quadratures of mode a_1 and mode a_2 as

$$\Delta a_+^2 \Delta a_-^2 \geq \frac{1}{\kappa^2}\left[\gamma_3\left(\langle \hat{\sigma}_{22} \rangle - \langle \hat{\sigma}_{11} \rangle\right) + 4\right]^2, \tag{129}$$

$$\Delta b_+ \Delta b_-^2 \geq \frac{1}{\kappa^2}\left[\gamma_3\left(\langle \hat{\sigma}_{33} \rangle - \langle \hat{\sigma}_{22} \rangle\right) + 4\right]^2. \tag{130}$$

Applying Eqs. (93), (94) and (95), we can write as

$$\Delta a_+^2 \Delta a_-^2 \geq f_{a_1}(\gamma_3), \tag{131}$$

$$\Delta b_+^2 \Delta b_-^2 \geq f_{a_2}(\gamma_3). \tag{132}$$

where

$$f_{a_1}(\gamma_3) = \frac{\left[\gamma_3 N(\eta^2 - 1) + 4(1 + \eta + 2N)((1+\eta)^2 + 3N\eta)\right]^2}{\kappa^2\left[(1 + \eta + 2N)((1+\eta)^2 + 3N\eta)\right]^2}, \tag{133}$$

$$f_{a_2}(\gamma_3) = \frac{\left[\gamma_3\left((1+\eta)^3 + N(1+\eta)(1+3\eta)\right) + 4(1+\eta+2N)((1+\eta)^2+3N\eta)\right]^2}{\kappa^2\left[(1+\eta+2N)((1+\eta)^2+3N\eta)\right]^2}. \tag{134}$$

Equations (133) and (134) attainable noise floors for the quadrature variance products of mode a_1 and mode a_2. Rather than fundamental commutation constraints, these state dependent bounds reflect the practical limits on squeezing imposed by the influx of reservoir fluctuations and atomic spontaneous emission. The variances of the plus and minus quadratures of mode a_1 and mode a_2 are expressible as

$$\Delta a_{\pm}^2 = \langle \hat{a}_{\pm}, \hat{a}_{\pm} \rangle, \tag{135}$$

$$\Delta b_{\pm}^2 = \langle \hat{b}_{\pm}, \hat{b}_{\pm} \rangle. \tag{136}$$

Now employing Eqs. (75) and (76), we have

$$\Delta a_{\pm}^2 = \frac{\gamma_3}{\kappa}\left(\langle \hat{\sigma}_{11} \rangle + \langle \hat{\sigma}_{22} \rangle\right) + \frac{4}{\kappa}(2N + 1 \pm 2M), \tag{137}$$

$$\Delta b_{\pm}^2 = \frac{\gamma_3}{\kappa}\left(\langle \hat{\sigma}_{22} \rangle + \langle \hat{\sigma}_{33} \rangle\right) + \frac{4}{\kappa}(2N + 1 \pm 2M). \tag{138}$$

Taking into account Eqs. (93), (94), and (95), the quadrature variances of mode a_1 and mode a_2 take the form

$$\Delta a_{\pm}^2 = \frac{\gamma_3\left[N(1+\eta)^2 + 4N^2\eta\right] + 4(2N+1\pm 2M)(1+\eta+2N)\left[(1+\eta)^2+3N\eta\right]}{\kappa(1+\eta+2N)\left[(1+\eta)^2+3N\eta\right]}, \tag{139}$$

$$\Delta b_{\pm}^2 = \frac{\gamma_3\left[(1+\eta)^3 + N(1+6\eta+5\eta^2) + 4N^2\eta\right] + 4(2N+1\pm 2M)(1+\eta+2N)\left[(1+\eta)^2+3N\eta\right]}{\kappa(1+\eta+2N)\left[(1+\eta)^2+3N\eta\right]}. \tag{140}$$

The uncertainty products shown in Fig. 11 and Fig. 12 exhibit three distinct dynamical regimes an initial decrease, a nonlinear curved increase, and a quasi-linear asymptotic growth arising from the competition between reservoir-induced quantum correlations and atom-induced noise processes. At low values of the stimulated-emission decay constant, γ_3, the uncertainty products remain close to their minimum values. This regime corresponds to strong quadrature squeezing generated by the two-mode squeezed-vacuum reservoir. The nonclassical correlations introduced by the reservoir are associated with the $-2M$ contribution appearing in the numerators of the minus quadrature variances, Δa_-^2 and Δb_-^2. These correlations suppress phase-sensitive quantum fluctuations below the standard vacuum limit, thereby reducing the uncertainty products and enhancing the squeezing characteristics of the cavity modes. As γ_3 increases, the uncertainty products exhibit a pronounced upward curvature, physically, the cascade three-level atom simultaneously acts as a gain medium and an internal source of quantum noise. Although stimulated emission enhances intracavity photon generation, spontaneous-emission processes associated with the atomic decay rate γ introduce additional fluctuations. Consequently, higher-order nonlinear contributions, such as the η^2 terms in Eq. (139) and the $(1+\eta)^3$ dependence in Eq. (140), become increasingly significant. These terms represent multiphoton noise-transfer and scattering mechanisms that progressively degrade the reservoir-induced squeezing and increase the uncertainty products. In the strong-coupling limit ($\eta \gg 1$), the highest-order terms dominate the system dynamics. In this regime, spontaneous-emission noise overwhelms the squeezing-induced noise suppression provided by the reservoir. As a result, the generalized uncertainty bounds, f_{a_1} and f_{a_2}, as well as the corresponding uncertainty products, increase along a quasi-linear asymptotic trajectory, indicating the gradual loss of nonclassicality and the onset of cavity-mode thermalization. A comparison between mode a and mode b reveals a pronounced quantum-optical asymmetry. The generalized uncertainty bound for mode a, $f_{a_1}(\gamma_3)$, exhibits a relatively moderate dependence on γ_3, scaling primarily through terms proportional to $N(\eta^2-1)$. In contrast, the bound for mode b, $f_{a_2}(\gamma_3)$, contains substantially stronger nonlinear contributions, including $(1+\eta)^3$ and $N(1+6\eta+5\eta^2)$, this difference explains the steeper growth observed in Fig. 12 relative to Fig. 11.

From a physical standpoint, mode b inherits fluctuations generated during the upper atomic transition before its own emission process occurs. Consequently, noise accumulated in mode a propagates through the cascade pathway and is transferred to mode b, making the lower-transition mode substantially more vulnerable to decoherence. This mechanism causes mode b to lose its squeezing properties at significantly lower values of γ_3 than Mode a. A key finding of this work is the derivation of dynamic, attainable noise floors for an open quantum system. Unlike ideal canonical systems where the standard quantum limit is fixed purely by fundamental commutation relations, the effective lower

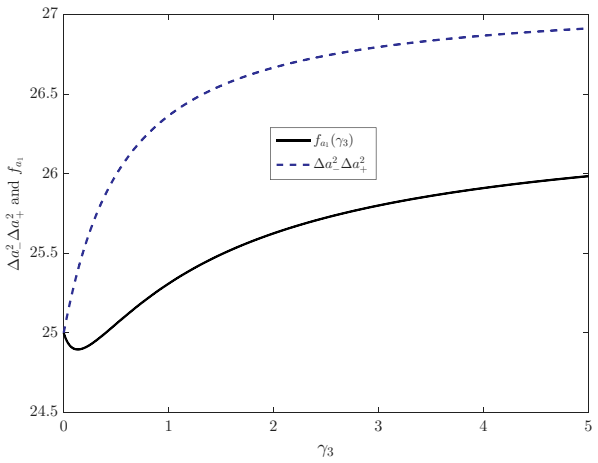


FIG. 11: Plots of $\Delta a_-^2 \Delta a_+^2$ of [Eq. (139)] and $f_{a_1}(\gamma_3)$ of [Eq. (133)] versus γ_3 for $\kappa = 0.8$, $\gamma = 0.4$ and $r = 0.5$.

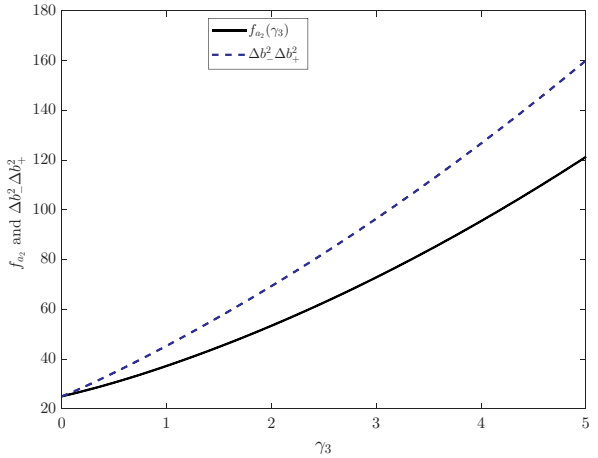


FIG. 12: Plots of $\Delta b_-^2 \Delta b_+^2$ of [Eq. (140)] and $f_{a_2}(\gamma_3)$ of [Eq. (134)] versus γ_3, for $\kappa = 0.8$, $\gamma = 0.4$ and $r = 0.5$.

bounds $f_{a_1}(\gamma_3)$ and $f_{a_2}(\gamma_3)$ increase dynamically with the effective atom-cavity coupling. This result reveals that the practical limit on achievable continuous-variable squeezing is dictated by the complex interplay between engineered reservoir fluctuations and the active atomic gain medium, which introduce unavoidable dissipation and higher-order noise. Recent studies have shown that squeezed-vacuum reservoirs can efficiently generate continuous-variable squeezing, entanglement, and quantum steering in cavity and optomechanical systems[24],[27],[28]. Consistent with these findings, the present model exhibits strong nonclassical behavior in the weak-coupling regime. However, our results uncover a previously unexplored limitation: the cascade three-level atomic medium introduces higher-order nonlinear noise channels that fundamentally restrict the preservation of nonclassical correlations. In particular, the strong nonlinear scaling observed for mode b, exemplified by the $(1+\eta)^3$ dependence, demonstrates that the atomic cascade structure itself imposes an intrinsic upper bound on achievable squeezing. Therefore, realizing robust quantum resources for quantum communication and continuous-variable quantum information processing requires careful optimization of γ_3, balancing gain enhancement against the detrimental effects of spontaneous-emission-induced noise.

1.5. Conclusion

In conclusion, we have shown that the interplay between a two-mode squeezed-vacuum reservoir and a cascade three-level atomic system provides an effective mechanism for tailoring photon statistics and nonclassical properties in a bimodal cavity. Our analysis reveals two distinct operational regimes governed by reservoir-induced correlations and atom–cavity interactions. In the strong-squeezing regime, photon generation, intracavity intensity, and intermodal correlations are primarily controlled by correlated photon-pair injection and the suppression of vacuum fluctuations. In contrast, increasing the stimulated-emission decay constant strengthens nonlinear gain, promotes asymmetric photon populations, and gives rise to sequential emission dynamics inherent to the cascade configuration.

A notable result is the simultaneous manifestation of continuous-variable quantum effects, such as squeezing and entanglement, alongside discrete-variable features, including photon antibunching. Furthermore, the analytical derivation of state-dependent noise floors demonstrates that practical squeezing limits in open quantum systems are

dynamically shaped by dissipative system-reservoir interactions. The reduction of squeezing at strong coupling identifies higher-order atomic noise processes as a fundamental limitation on quantum-state engineering[29]. Overall, the proposed system offers versatile and tunable control over photon intensity, correlations, and quantum fluctuations, making it a promising platform for generating engineered nonclassical light for quantum communication, precision metrology, and continuous-variable quantum information technologies.

Declaration of competing interest

The authors declare that they have no known financial or personal relationships that could have potentially influenced the work reported in this paper.

Data availability

No data was used for the research described in the article.

CRediT authorship contribution statement

AdagnAddisuDabulo, *MisrakGetahun*: Writing review, editing, Writing original draft, Visualization, Software, Resources, Methodology, Investigation, Formal analysis, Conceptualization.

Funding

This research received no external funding. The authors are employed by Hawassa University, which provided salary support but had no role in the design of the study, data analysis, interpretation, or writing of the manuscript.

References

[1] Fesseha K 1998 *Opt. Commun.* **156** 145
[2] Tesfa S 2020 *Quantum Optical Processes: From Basics to Application*
[3] Drummond P D and Reid M D 1990 *Phys. Rev. A* **41** 3930
[4] Sabri N H *Nonclassical Properties of Light in Atom-Cavity Interaction Scheme with Time and Intensity-Dependent Coupling*
[5] Daniel B and Fesseha K 1998 *Opt. Commun.* **151** 384
[6] Teklu B 2006 *Opt. Commun.* **261** 310
[7] Tesfa S 2008 *Eur. Phys. J. D* **43** 335
[8] Mebrahtu A 2005 *J. Mod. Opt.* **52** 813
[9] Collett M J and Gardiner C W 1984 *Phys. Rev. A* **30** 1386
[10] Lugiato L A and Strini G 1982 *Opt. Commun.* **41** 67
[11] Deng H, Erenso D, Vyas R and Singh S 2001 *Phys. Rev. Lett.* **86** 2770
[12] Milburn G J and Walls D F 1981 *Opt. Commun.* **39** 401
[13] Anwar J and Zubairy M S 1994 *Phys. Rev. A* **49** 481
[14] Reid M D and Drummond P D 1988 *Phys. Rev. Lett.* **60** 2731
[15] Lloyd S and Braunstein S L 1999 *Phys. Rev. Lett.* **82** 1784
[16] Nieves Gonzlez Y A *Third-Order Frequency-Resolved Photon Correlations from a Single Quantum Dot's Resonance Fluorescence*
[17] Breuer H-P and Petruccione F 2002 *The Theory of Open Quantum Systems* (Oxford: Oxford University Press)
[18] Gu X, Kockum A F, Miranowicz A, Liu Y X and Nori F 2017 *Phys. Rep.* **718** 1
[19] Toyli D M *et al.* 2016 *Phys. Rev. X* **6** 031004
[20] Koch J *et al.* 2007 *Phys. Rev. A* **76** 042319
[21] Murch K W *et al.* 2013 *Nature* **502** 211
[22] Ldge S 2016 *New J. Phys.* **18** 063011
[23] Guo Y, Zhang J, Guo X and Xiao L 2023 *New J. Phys.* **25** 083023
[24] Salih E and Getahun M 2025 *Two-mode light in optomechanical cavity with squeezed vacuum reservoir* **15** 1
[25] Loudon R 2000 *The Quantum Theory of Light*, 3rd edn (Oxford: Oxford University Press)
[26] Guo Y, Zhang H, Guo X, Zhang Y and Zhang T 2022 *Opt. Express* **30** 8461
[27] Salih E and Getahun M 2025 *Results in Optics* 100909. doi:10.1016/j.rio.100909
[28] Mussie A and Getahun M 2025 *Results in Optics* 100840. doi:10.1016/j.rio.2025.100840
[29] Clerk A A, Devoret M H, Girvin S M, Marquardt F and Schoelkopf R J 2010 *Rev. Mod. Phys.* **82** 1155